

**NASA TECHNICAL  
MEMORANDUM**

Report No. 53841

**CASE FILE  
COPY**

**EXPERIMENTAL STUDY OF THE RESPONSE OF A STATIC  
LIQUID-VAPOR INTERFACE AFTER A SUDDEN  
REDUCTION IN ACCELERATION**

By Leon J. Hastings  
Astronautics Laboratory

June 26, 1969

**NASA**

*George C. Marshall Space Flight Center  
Marshall Space Flight Center, Alabama*



Page Intentionally Left Blank



## TABLE OF CONTENTS

	Page
SUMMARY .....	1
INTRODUCTION .....	2
EXPERIMENTAL HARDWARE .....	3
General Facility Description .....	3
Experimental Package .....	3
TEST PROCEDURES .....	5
Package Preparations .....	5
Data Reduction Procedures .....	6
Experimental Error .....	6
Prototype Simulation .....	6
EXPERIMENTAL RESULTS .....	9
Interface Shapes in a Cylinder .....	10
Interface Shapes in a Sphere .....	14
CONCLUSIONS AND RECOMMENDATIONS .....	16
APPENDIX .....	19
REFERENCES .....	21



# LIST OF ILLUSTRATIONS

Figure	Title	Page
1	Marshall Space Flight Center Drop Tower Facility .....	22
2	Experimental Drop Tower Package .....	23
3	Model Saturn V/S-IVB Propellant Containers .....	24
4	Experimental Interface Shapes in a Cylinder at Bond Number = 48 .....	25
5	Experimental Interface Shapes in a Cylinder at Bond Number = 48 .....	26
6	Experimental Interface Shapes in a Cylinder at Bond Number = 80 .....	27
7	Experimental Interface Shapes in a Cylinder at Bond Number = 94 .....	28
8	Measured Displacement of Interface Centerpoint in a Cylinder Versus Time .....	29
9	Measured Interface Oscillatory Magnitudes in a Six-Inch Diameter Cylinder .....	30
10	Measured Times Characteristic of Interface Formation Dynamics in a Six-Inch Diameter Cylinder .....	31
11	Oscillation Cycles Required for Interface to Attain Quasi-Equilibrium in a Six-Inch Diameter Cylinder .....	32
12	Total Time Required for Interface to Attain Quasi-Equilibrium in a Six-Inch Diameter Cylinder .....	32
13	Nondimensionalized Interface Oscillation Period in a Cylinder Versus Bond Number .....	33

## LIST OF ILLUSTRATIONS (Concluded)

Figure	Title	Page
14	Nondimensionalized Time Required for Interface to Attain Quasi-Equilibrium in a Cylinder Versus Bond Number .....	34
15	Experimental Interface Formation Dynamics Characteristic of a Sphere at Bond Number = 80 .....	35
16	Experimental Interface Formation Dynamics Characteristic of a Sphere at Bond Number = 80 .....	36
17	Experimental Interface Shapes in a Spherical Segment at Bond Number = 80 .....	37-40
18	Experimental Interface Shapes in a Spherical Segment at Bond Number = 80 .....	41
19	Thrust Nozzle Calibration Curve .....	42

## TABLES

Table		Page
I	Equilibrium Interface Scaling Parameters .....	8
II	Measured Interface Oscillation Characteristics in a Spherical Segment .....	16



## LIST OF SYMBOLS

Symbol	Definition
$a$	Local acceleration, $\text{ft}/\text{sec}^2$
$B_N$	Bond number based on container radius
$D$	Container diameter, ft
$g_o$	Dimensional constant, $\text{lb}_m\text{-ft}/\text{lb}_f\text{-sec}^2$
$H$	Vertical displacement of interface centerpoint, ft
$H_o$	First interface overshoot depth, ft
$H_1$	Second interface overshoot depth, ft
$n$	Number of oscillation cycles
$R$	Container radius, ft
$t_o$	Time of first interface overshoot, sec
$t_p$	Oscillation period, sec
$\bar{t}_p$	Nondimensionalized oscillation period
$t_t$	Total damping time, sec
$\bar{t}_t$	Nondimensionalized damping time
$Z$	Vertical distance, ft
$\beta$	Empty fraction
$\delta$	Damping decrement
$\sigma$	Surface tension, $\text{lb}_f/\text{ft}$



EXPERIMENTAL STUDY OF THE RESPONSE  
OF A  
STATIC LIQUID-VAPOR INTERFACE  
AFTER A SUDDEN REDUCTION IN ACCELERATION

SUMMARY

The dynamics associated with the formation of low-gravity equilibrium liquid-vapor interfaces after a sudden reduction in acceleration were experimentally investigated. The Marshall Space Flight Center (MSFC) drop tower facility was used to obtain low-gravity durations of up to 4.3 seconds. Tests were conducted in 1/43 scale S-IVB liquid hydrogen and oxygen tanks using petroleum ether, a zero contact angle liquid, as the test fluid. The hydrogen tank was a six-inch diameter cylinder and the oxygen tank was constructed from two spherical segments with three-inch radii.

The test data indicated that, except for very high Bond numbers (on the order of 400 or greater) and small fill levels in spherical or spheroidal containers, the time for a surface to attain complete equilibrium in containers about six inches or greater in diameter cannot be measured using drop tower testing. Secondary oscillation modes will persist throughout the test period and will exhibit negligible damping. However, results were obtained that enabled estimates to be made of the time required for a surface to attain a state of quasi-equilibrium.

Twenty-five tests were conducted using the cylindrical container and Bond numbers ranging from 24 to 94. The results indicated that the time required for the surface to attain quasi-equilibrium in a six-inch diameter cylinder is about 30 seconds and 3.25 seconds at Bond numbers of 24 and 94, respectively. The measured surface profile and oscillation amplitude data are presented in dimensionless form to permit application to other zero contact angle liquids and cylinder sizes. Also, empirical relations that approximate the surface period of oscillation and damping time were derived.

The surface formation characteristics observed in the model oxygen tank during four tests are presented. All four experiments were performed at a Bond number of 80, and the only test parameter varied was the empty fraction, or fill level. For liquid levels in the upper half of the container, the surface underwent the same type of oscillations observed in the cylindrical containers, except that the oscillations were magnified considerably. At fill levels in the lower half of the tank, however, the interface activity was very low. The small oscillations observed were not surprising, because the equilibrium surface



profiles did not differ greatly from the normal gravity configurations. The estimated times required for the surface to attain equilibrium were eighteen seconds and two seconds for empty fractions\* of .056 and .92, respectively.

It can be generally stated that, for a given container and liquid, the surface formation transients encountered in drop tower testing are a function of the low-gravity equilibrium surface curvature; that is, the higher the static surface curvature, the greater the oscillation magnitudes and duration.

## INTRODUCTION

The MSFC drop tower has been used primarily in support of the Saturn V lunar mission, which requires a third-stage (S-IVB) orbital coast period of approximately 4 1/2 hours prior to main engine restart. During the investigation of certain fluid behavior phenomena in the MSFC drop tower, difficulties were sometimes encountered in analyzing the data, because the dynamics of equilibrium liquid-vapor interface formation were superimposed on the dynamics of primary interest. Therefore, to assess the influence of these interface formation dynamics on other fluid behavior phenomena, a separate experimental study of interface formation transients was made.

The basic objectives of the program were to (1) assess the dynamics associated with interface formation in the model liquid hydrogen and oxygen tanks, (2) estimate the time required for the surfaces to attain quasi-equilibrium, and (3) present the data in general form so that it could be applied to other container sizes and zero contact angle liquids. Since the low-gravity behavior of liquid hydrogen in the S-IVB stage was of primary concern, this study emphasized cylindrical containers.

---

\* Gas volume to total volume ratio, assuming the spherical segment is a complete sphere.



## EXPERIMENTAL HARDWARE

### General Facility Description

The NASA-George C. Marshall Space Flight Center (MSFC) drop tower facility was used to obtain the experimental data presented in this report. Like most drop towers used for studying the effects of weightlessness or low gravity, the MSFC facility consists of three major components; an experimental package that contains the test specimen and all necessary instrumentation, an aeroshield that provides a protective environment for the test package, and a deceleration device that catches and safely stops the test package/aeroshield combination. A description of the facility and its operation is documented in References 1 and 2. The facility and its capabilities are shown in Figure 1.

The tower is located in the Saturn V dynamic test stand, which provides a drop distance of 294 feet and allows a maximum low-gravity data period of about 4.3 seconds. The experimental package is completely self-supporting and operates independently of the aeroshield during the test period. The package contains an air thruster system, and by using various pressure levels and thrust nozzles, constant accelerations from  $.001 g_0$  to  $.05 g_0$  can be obtained on the package. Because the aeroshield and test package fall at different rates, the aeroshield contains an 8-foot high bay to allow package motion within the aeroshield. To control the relative displacement between the aeroshield and test package, a thruster system capable of positive or negative thrust is mounted on the aeroshield. Also, an aerodynamic drag plate is sometimes used to increase the drag coefficient and, thereby, reduce the thrust required to control the relative motion of the aeroshield/package.

The aeroshield is guided by vertical rails into the deceleration device, a tube 40 feet long that depends upon the pneumatic forces provided by atmospheric air to safely terminate the aeroshield momentum at the end of a drop.

### Experimental Package

The major components of an experimental package used to acquire data on equilibrium interface formation are identified in Figure 2. The more significant package components and their capabilities and functions are described below.



Frame - The basic package structure consists of an open rectangular parallelepiped (36 in. x 36 in. x 18 in.) constructed from aluminum angle with an aluminum plate for the floor.

Thruster System - The thruster system consists of a pressure bottle, an adjustable regulator, a solenoid shutoff valve, a pressure transducer, a sonic nozzle, and a fill-and-drain valve. The desired thrust level is produced by exhausting compressed gaseous nitrogen through the nozzle at a pressure determined from a nozzle calibration curve of thrust versus pressure. The proper flowrate is set before the test by adjusting the regulator. The line pressure during the test is monitored by the pressure transducer.

Model Containers - The containers are geometrically scaled (1/43) Saturn V third-stage propellant tanks (liquid hydrogen and oxygen). The tanks are constructed of Plexiglas as described in Figure 3.

Instrumentation - With the exception of the movie camera, all instrumentation on the package is recorded using an on-board telemetry system. The present system has eight channels for recording and transmitting calibrated signals from the various instrumentation on board the package. Each pertinent source of instrumentation is discussed below.

Camera: The primary source of data is the 16mm movie camera that photographs liquid behavior in the test container during the test. The camera is capable of 400 frames per second and applies coded time "blips" to the film so that the liquid motion can be correlated with other test events. The camera also photographs a grid painted on the aeroshield wall so that the relative position of the package in the aeroshield can be monitored during the test drop.

Pressure Transducer: A pressure transducer that measures within  $\pm 1\%$  actual pressures is used to monitor line pressure at the thrust nozzle entrance during the test. The transducer permits the detection of any undesirable flow transients and provides a means of calculating the acceleration on the package.

Low-gravity Accelerometer: The primary functions of this accelerometer are to monitor objectionable perturbations to the experi-



ment and to measure the low-gravity time period. Its secondary function is to provide a backup measurement of package acceleration. The accelerations indicated by the accelerometer are usually within 15% of those calculated from the thrust system; however, the calculated accelerations are accepted as correct in this study because:

(a) The thrust system calibration of thrust versus line pressure can be determined with proven accuracies and methods. Also, a sizeable error in line pressure must exist before a significant variation in package acceleration is created.

(b) The accelerometer occasionally contradicted itself, indicating that the same acceleration existed on some tests while both the fluid motion and nozzle pressure indicated otherwise. Subsequent drop tower testing proved that the accelerometer had not been properly calibrated during the "Interface Shape" tests.

(c) The accelerometer was not operational during early phases of the drop tower program when much of the interface shape data were taken.

Control System - A timer sequences and controls the functions of the package. On the "interface package", the timer controls the thrust system, camera, lights, and a pulse generator that delivers a 10, 100, or 1000 cps signal to the camera.

## TEST PREPARATIONS AND PROCEDURES

### Package Preparations

To prevent the package from tilting during drop tests, the package was balanced as accurately as possible about the vertical axis of the thrust nozzle so that the thrust would be through the center of gravity of the package. After all masses on the package were prepared for testing, the package was balanced using a strain-gage balancing table that located the package center of gravity within  $\pm .003$  inches of the thrust axis.



## Data Reduction Procedures

Experimental data acquired using the drop tower facility were reduced to useable form with the following procedures.

Telemetry Data - All telemetry data were stored on magnetic tape and made available in strip chart plots as well as in print-out form.

Camera Data - Prior to testing, the Plexiglas tank was calibrated for distortion by inserting a grid pattern of known dimensions inside the container and photographing the grid with and without the test liquid in the container. The calibration photography was accomplished with the same camera lens, distance from camera to the test specimen, etc., as were used in the actual experiments. The apparent and actual grid dimensions were stored on a computer tape so that when the interface profile dimensions were recorded with a "Teleredex" film reader, the measured dimensions could be automatically corrected for distortion before the data were plotted in graphical form.

## Experimental Error

The magnitude of error entailed in acquiring experimental interface configuration data, using the test apparatus just described, is dependent on two basic factors: test package acceleration accuracy and visual distortion of the interface profile. Estimates of the degree of error for each source of deviation included in these two categories are enumerated in the Appendix. It was concluded that the greatest source of error resulted from the reflections, distortions, shadows, etc. that occurred whenever the low-gravity surface took shape.

## Prototype Simulation

The conditions applicable to the space vehicle design problems under investigation at MSFC had to be simulated in the drop tower experiments. The simulation of prototype conditions pertaining to static equilibrium surface configurations required that Bond number, a contact angle of zero degrees, and container geometry be properly scaled. The prototype Bond numbers (based on tank radius) are 80 and 240 for the liquid hydrogen and liquid oxygen (LOX) tank respectively. At the



time this study was performed, however, the propellant behavior in the hydrogen tank was of primary interest, and therefore only preliminary testing at a convenient Bond number was conducted with the LOX tank.

The scaling criteria were met by using petroleum ether as the test fluid. Since there are many types of petroleum ether, the viscosity, surface tension, and density of the specific type used were measured by the Chemistry Branch of the Astronautics Laboratory, MSFC. The petroleum ether/Plexiglas contact angle was so small that it could not be measured. In addition, the petroleum ether exhibited a high degree of "spreadability" on the Plexiglas. Therefore, it was concluded that petroleum ether would satisfy the zero contact angle criteria.

The measured petroleum ether properties and the prototype and model scaling parameters are listed in Table I using a Bond number of 80 as an example.



TABLE I. EQUILIBRIUM INTERFACE SCALING PARAMETERS

	Prototype System		Model
	Liq. Hydrogen	Liq. Oxygen	**Pet. Ether
*Viscosity, (lbm/Ft-Sec)	$1.1 \times 10^{-5}$	$1.3 \times 10^{-4}$	$1.67 \times 10^{-4}$
Density, $(\frac{1b_f \text{ Sec}^2}{ft^4})$	.137	2.21	1.23
Surface Tension, (lb <sub>f</sub> /ft)	$1.62 \times 10^{-4}$	$9. \times 10^{-4}$	$1.02 \times 10^{-3}$
Kinematic Surface Tension, (ft <sup>3</sup> /sec <sup>2</sup> )	$1.2 \times 10^{-3}$	$4.06 \times 10^{-4}$	$8.3 \times 10^{-4}$
Acceleration Level, a/g <sub>0</sub>	$2.6 \times 10^{-5}$	$8.6 \times 10^{-6}$	.033
Tank Radius, R (ft)	10.8	10.8	.25
Contact Angle, (Deg)	0	0	0
Bond Number, B <sub>N</sub>	80	80	80

\* As discussed in a subsequent section, capillary forces dominate viscous effects in containers of practical significance. Therefore, the model viscosity need only be in the same range as that of the prototype.

\*\*Properties at 70°F.

## EXPERIMENTAL RESULTS

The preliminary experimental investigation of equilibrium liquid surface configurations in low-gravity environments was conducted in the MSFC drop tower using two container shapes, a cylindrical and a spherical segment (refer to Figure 3). Theoretical interface shapes were determined utilizing the procedure outlined in Reference 3 and were compared with the measured data. As mentioned previously, however, the primary objective of these drop tower tests was not to verify the theoretical static interface configurations (such a verification can be accurately obtained by inexpensive and less complicated methods\*), but rather, to make some general observations concerning the equilibrium interface formation transients that are inherent in drop tower studies.

It has been proven (both experimentally and theoretically) that if a liquid-vapor system is subjected to a sudden decrease in acceleration level, such as that encountered in drop tower investigations, certain interface oscillations must occur before the equilibrium configuration is attained.

During drop tower testing in other areas of concern, such as liquid draining and slosh in near weightless environments, it is desirable that these interface formation transients dissipate before the acquisition of data is initiated. In practically all cases, however, the maximum test time available on the MSFC drop tower (4.3 seconds) is insufficient to permit the interface to attain equilibrium. As a result, the interface formation transients are often superimposed on the liquid dynamics under investigation. Thus, proper analysis of low-gravity liquid dynamics in the drop tower requires an understanding of the interface formation transients.

---

\* Such methods include liquid-liquid models and a modification of the Hele-Shaw Cell, which are outlined in References 4 and 5, respectively.



According to available literature, the response of a static liquid to a sudden decrease in acceleration\* has been investigated only for conditions where the liquid-vapor system is suddenly transitioned from a state of high acceleration to weightlessness. A major objective of the MSFC interface shape drop tower tests was to investigate the effects of low gravity, as opposed to zero gravity, on the subject interface transients.

### Interface Shapes in a Cylinder

Twenty-five drop tower tests were conducted to observe interface formation in the six-inch diameter cylindrical container at Bond numbers ranging from 24 to 94. Some observations on general interface behavior, correlation of experimental with theoretical data, and time for the interface oscillations to dampen are outlined in subsequent paragraphs.

General Interface Behavior - Significant oscillations of the interface were observed in all tests, and although the interface oscillation magnitudes and frequency were a function of Bond number, the same general behavioral pattern appeared in all of the tests performed. Some of the shapes assumed by the interface are pictorially illustrated in Figure 4, which are photographs from a typical test at a Bond number of 48.

Theoretical and Experimental Interfaces - Although a major portion of the experimental interface usually oscillated throughout a test, the interface curvature near the container walls appeared to agree rather well with the theoretical shape in that same region during a significant portion of each test period. At times the entire interface matched the theoretical configuration reasonably well. The type of correlations obtained are illustrated in Figures 5 through 7 where the calculated interfaces are superimposed on data plots of the experimental shapes from representative tests. Deviations of the measured interfaces from the theoretical interfaces can be attributed to the experimental surface oscillations and distortion.

---

\* References 6 and 7 propose theoretical explanations of these interface oscillations. An experimental evaluation of the phenomena is presented in Reference 8.



Interface Dynamics - A study of the experimental data was made to obtain an estimate of time for the interface oscillations to dampen to a state reasonably close to that of static equilibrium, that is, quasi-equilibrium. Since the interface deviation from its static shape was greatest at the interface centerpoint, the activity of this centerpoint (sometimes termed "interface overshoot") should provide a measure of the time for an interface to approach equilibrium. The interface centerpoint as a function of time was read for each test, and representative results are presented in Figure 8. These centerpoint readings show, as did the 16mm movies, that several vibrational modes existed in each test. Such behavior is not surprising, because a low-gravity surface is analogous to a bubble that always exhibits many vibrational modes.

Assuming that the primary vibrational mode of the surface formation transients is represented by the interface centerpoint oscillations, the frequency and magnitude of the "overshoot" were used to estimate the primary period of oscillation and the damping decrement, respectively, where overshoot depth was measured from the normal gravity liquid level. These measured amplitudes and oscillation periods were then used to estimate the period of time required for the surface to attain quasi-equilibrium. The relations used in the analysis are as follows:

If  $\delta = \ln \frac{H_0}{H_1}$  where  $H_0$  is the first maximum amplitude and  $H_1$  the second, it is easily shown that:

$$n = 1/\delta \ln (H_0/H_n) \quad (1)$$

where  $n$  is the number of cycles required for the first amplitude to diminish to a magnitude corresponding to the interface static position ( $H_n$ ).

A maximum of two overshoots, and in many cases only one, occurred during a test due to the limited low-gravity periods (2.5 to 4. seconds). The measured magnitudes of the first and second overshoots, represented by  $H_0/R$  and  $H_1/R$ , respectively, and the logarithmic damping decrement based on these measured oscillations are presented in Figure 9 as a function of Bond number. Figure 10 presents the measured periods characteristic of the surface oscillations, that is,



the time from test initiation to the first maximum oscillation,  $t_o$ , and the period between the first and second oscillations,  $t_p$ , as functions of Bond number.

Figures 9 and 10 illustrate that the oscillation magnitude and period decrease almost linearly with decreasing Bond number over a range from 48 to 94. Five tests were not within this Bond number range; one test was conducted at a Bond number of 24 and four tests at a Bond number of 33. Although only one oscillation could be observed in these tests, the time of the first oscillation,  $t_o$ , should be indicative of the oscillation period,  $t_p$ . The ratio of these two characteristic times,  $t_p/t_o$ , for the other tests indicated no dependence on Bond number and for all practical purposes was constant (ranged from 1.85 to 1.92). Therefore, using an average  $t_p/t_o$  ratio of 1.89 and the measured  $t_o$  for Bond numbers of 24 and 33, oscillation periods were calculated and are presented as extrapolated data points.

Figure 11 presents the number of cycles,  $n$ , required for the oscillations to approach equilibrium. It is apparent that the damping effect of acceleration rapidly increases above Bond numbers of 80 and that no more than one cycle should be required for the primary oscillations to dampen above Bond numbers of 100.

Note that data concerning the oscillation period (Figure 10) yielded relatively good repeatability, while data on the oscillation magnitudes indicated some scatter (Figure 9). It is assumed, therefore, that the oscillation magnitudes were sensitive to factors other than acceleration level variation. Although care was taken to maintain clean test container surfaces, it is suspected that the rate of wetting (spreadability) differed somewhat from test to test and affected the oscillation magnitudes.

Finally, using the data presented in Figures 9 through 11, the total time,  $t_t$ , required for the dynamics to dampen to a state of quasi-equilibrium was estimated where:

$$t_t = t_o + n t_p \quad (2)$$

and the results are presented in Figure 12. Note that this damping time, as well as the other surface formation time data presented thus



far, does not reflect the effects of container size and fluid property variations. That is, the Bond number is not an adequate scaling parameter for interface dynamics. These effects were not investigated in the MSFC test program; however, other investigators of liquid surface responses (References 8 and 9) have shown that interface oscillations are related to fluid properties and container diameter (D) by the following relation:

$$\text{Oscillation Period} \approx \left( \frac{\rho}{\sigma} \right)^{1/2} (D)^{3/2} \quad (3)$$

Equation (3) does not consider viscous effects; however, References 9 and 10 indicate that the influence of viscosity, in comparison with surface tension, is negligible for containers of practical sizes.

Using equation (3) to non-dimensionalize the measured surface response times, the MSFC experimental data can then be scaled to various zero-degree contact angle fluids and cylindrical containers. The non-dimensionalized versions of the oscillation period,  $t_p$ , and damping time,  $t_t$ , are presented in Figures 13 and 14, respectively, as a function of Bond number and are defined by the empirical relations:

$$\bar{t}_p = \frac{t_p}{(\rho/\sigma)^{1/2} (D)^{3/2}} = \frac{.847}{(B_N)^{.39}} \quad (4)$$

$$t_t = \frac{t_t}{(\rho/\sigma)^{1/2} (D)^{3/2}} = \frac{6.12}{.0345 B_N} \quad (5)$$

The usefulness of Figures 13 and 14 or relations (4) and (5) are illustrated in the following examples:

a. If a drop tower test objective requires that a petroleum ether surface attain quasi-equilibrium within two seconds after test initiation at a Bond number of 80, then a container diameter of about 3.4 inches would be necessary. An oscillation period of .8 seconds would occur in the test.

b. In a full-scale vehicle, an oscillation period of 445 seconds would exist in a 260-inch diameter container of liquid hydrogen at a Bond number of 80, and about 1,130 seconds would be required for the interface to attain quasi-equilibrium after injection into the low gravity environment.



## Interface Shapes in a Sphere

As mentioned earlier, interface characteristics were observed in a model liquid oxygen tank for the third stage of the Saturn V space vehicle. Although the tank is constructed from two spherical segments, there is no reason the interface shape data cannot be applied to a spherical container if the juncture of the spherical segments is not allowed to interfere with the capillary effects.

Only precursory testing has been completed with the model liquid oxygen tank, and therefore, experimental results from only four tests are presented. All four experiments were performed at a Bond number of 80 and a single test parameter, the empty fraction, was varied. The data available did, however, provide some informative results concerning interface behavior upon the removal of normal gravity.

General Observations - For liquid levels in the upper half of the container, the interface seemed to undergo the same type of oscillations as those observed in the cylindrical tanks, except that the oscillation magnitudes were increased significantly. Photographs that depict these oscillations are presented in Figure 15. Note that the depth of the initial interface overshoot was such that the hydraulic pressure caused the overextended interface to rapidly contract and trap a vapor bubble within the liquid. It should also be noted that a "blind spot" exists in the test tank at the tank juncture (horizontal centerline), and therefore, the interface in this region of the tank is not actually flat, although it appears to be in the photographs.

At fill levels in the lower half of the tank, however, the interface activity was very low. The small oscillations observed were not surprising, because the theoretical interfaces predicted for this region of a sphere at Bond number = 80 did not greatly deviate from the normal gravity configurations. The maximum interface overshoot from one of these tests is pictorially represented in Figure 16.

Theoretical and Experimental Interface - Two tests were conducted at a fill level which corresponds to an empty fraction ( $\beta$ ) of .056 in a sphere. The experimental interface profiles measured from one of the tests\* are shown in Figure 17 for various times during the test.

---

\* Results from the two tests at this fill level were practically identical.



As in the cylinder, the theoretical shape superimposed on the data correlates reasonably well with the interface curvature near the container boundary, and the interface as a whole seems to oscillate about the calculated static configuration. Some difficulties were encountered in tracing the interface shapes, because the distortion problems created by the optical lens effect of the container were enhanced by the complex interface configurations and reflections. These outlines can be examined in the experiment photographs.

Experimental data from tests with fill levels in the lower half of the container ( $\beta = .92$  and  $.9$ ) are presented in Figure 18. Since the interface deviated slightly from its normal gravity position and most of the curvature existed very near the container boundary, distortion made accurate readings impossible. However, the data shown seems to verify the theoretical interface rise at the tank walls.

Interface Dynamics - As in the tests with the cylinder, interface oscillations were measured at the surface centerpoint and the data acquired are shown in Table II. The oscillation magnitudes were small and, therefore, difficult to assess for the two tests with fill levels in the lower half of the container. One small overshoot was observed in the test with an empty fraction of  $.92$ . A second oscillation could not be definitely discerned, hence, neither a period of oscillation nor damping time was estimated. The surface did appear to attain quasi-equilibrium about two seconds after test initiation. Practically no motion was evident in the test with an empty fraction of  $.99$ , because the equilibrium configuration varied insignificantly from its normal gravity shape.



TABLE II. MEASURED INTERFACE OSCILLATION CHARACTERISTICS IN A SPHERICAL SEGMENT

MEASURED DATA	*EMPTY FRACTION			
	.056	.056	.92	.99
First Overshoot Amplitude, $H_0/R$	.5	.5	.02	0
Second Overshoot Amplitude, $H_1/R$	.3	.3	0	0
First Overshoot Time, $t_0$ (sec)	.85	.85	.59	
Oscillation Period, $t_p$ (sec)	2.24	2.25	Not Avail.	
Cycles Required to Damp to Quasi-Equilibrium, $n$	7.7	7.7	1.	0
Time Required to Attain Quasi-Equilibrium, $t_t$ (sec)	18	18	2.	0

\* This empty fraction is that corresponding to a sphere.

## CONCLUSIONS AND RECOMMENDATIONS

Based on the theoretical and experimental data acquired by this and other investigators, the following conclusions and recommendations are made:

### Conclusions

1. Accurate equilibrium surface configurations are often difficult to obtain in a drop tower facility, especially in containers on the order of six inches in diameter, because of the interface formation transients that occur whenever the acceleration is suddenly reduced.

2. Except for very high Bond numbers and small fill levels in spherical or spheroidal containers, the time for a surface to attain complete equilibrium in containers on the order of six inches or greater in diameter cannot be measured using drop tower testing, because



secondary oscillation modes will persist throughout the test period and will exhibit negligible damping. However, the time for the surface to achieve quasi-equilibrium can be estimated based on measurements of the primary oscillation mode or interface "overshoot."

3. In a six-inch diameter cylinder, a zero contact angle liquid will attain quasi-equilibrium in approximately 30 seconds and 3.25 seconds at Bond numbers of 24 and 94, respectively. The primary oscillation mode periods for Bond numbers of 24 and 94 are 2.9 and 1.7 seconds, respectively.

4. In nondimensionalized form, the empirical relations describing the surface oscillation period and damping time required to attain quasi-equilibrium are:

$$\bar{t}_p = 8.98/B_N^{.36} \quad \text{and} \quad \bar{t}_t = 6.12/\epsilon^{.0345} B_N$$

5. In a six-inch diameter sphere, a zero contact angle liquid at a Bond number of 80 will attain quasi-equilibrium in about 18 seconds for an empty fraction of .056 and 2 seconds for an empty fraction of .92. The oscillation period at an empty fraction of .056 is 2.25 seconds.

6. It can be generally stated that, for a given container and liquid, the surface formation transients encountered in drop tower testing are a function of the low-gravity equilibrium surface curvature; that is, the higher the curvature of the static surface the greater the oscillation magnitudes and duration.

7. Specifically, the static surface formation time is mainly a function of the following variables: liquid surface tension and density, contact angle, acceleration level, and (except for cylindrical containers), liquid fill level. With the exception of contact angle, these functions can be arranged in nondimensional form to enable scaling to various container sizes and liquids, but additional experimental verification of these nondimensional forms is advisable.

#### Recommendations

1. Low-gravity equilibrium interface shapes need not be experimentally determined in most cases, because the profiles can



usually be theoretically computed. If equilibrium surface configurations are desired for liquids in complex nonsymmetrical containers, then experimental determinations may be necessary. Drop tower testing is not recommended for such purposes, because the surface shapes can be more accurately determined with less expensive liquid-liquid model testing.

2. If, after a sudden reduction in acceleration level, the surface formation dynamics are of interest, drop tower testing is an excellent experimental method for investigating such phenomena.

3. Future experimentation concerning interface formation should include investigations of various container sizes and liquid/solid contact angles.



## APPENDIX

### EXPERIMENT ERROR

The primary sources of error and their estimated magnitudes are outlined in the following paragraphs.

#### Thrust Nozzle Calibration

The sonic nozzles were calibrated using a mockup of the experimental package thrust system. The apparatus was arranged so that the nozzle end of the tubing rested on a ground balance that was preloaded with certified scientific weights. By increasing or decreasing the line pressure until the weights were nulled, a calibration curve of nozzle thrust versus line pressure was generated. The line pressure was read with a "Hise" gauge that was calibrated to within  $\pm .1\%$ . The certified weights can be considered exactly correct. Using a 200 pound package as a standard of reference, the thrust levels in the experiments performed ranged from two to eight pounds force. Referring to Figure 19, it is readily apparent that a  $\pm .1\%$  error in pressures corresponding to the test package thrust range results in such a small thrust deviation that it can be considered negligible.

#### Measured Line Pressure on Package

The thrust pressure on the package is measured with a transducer which is accurate to within  $\pm 1\%$ . This variation could cause a maximum corresponding error of about  $\pm 1\%$  in acceleration.

#### Thrust Fluctuations

The flowrate through the thruster system is maintained to within  $\pm 2\%$  of the desired rate according to the regulator specifications. However, data from the line pressure gauge has indicated that this maximum deviation occurs only occasionally and that the pressure level does not cycle or oscillate (except for a very brief period after flow initiation) but varies almost linearly from test initiation to test termination.



## Visual Distortions

The method used in this investigation to account for visual distortion of dimensions within the Plexiglas container was virtually free of error for portions of the tank in which the calibration grid can be clearly photographed. However, a "blind spot" about .1 inches wide did exist in the containers at the wall, and therefore, measurements very near the boundaries were sometimes difficult to make.

In addition to the distortions caused by the Plexiglas/liquid combination, reflections and shadows were present whenever the low-gravity surface formed. Considerable difficulty was sometimes encountered, especially in the spherically-shaped container, in determining whether an outline represented the interface or was merely a shadow or reflection. Whenever this type of error was a factor, the plotted experimental interface profile appears slightly erratic. Also, to minimize the impact of such uncertainties, no attempts were made to trace portions of the surface that were indefinite.

## CONCLUSIONS

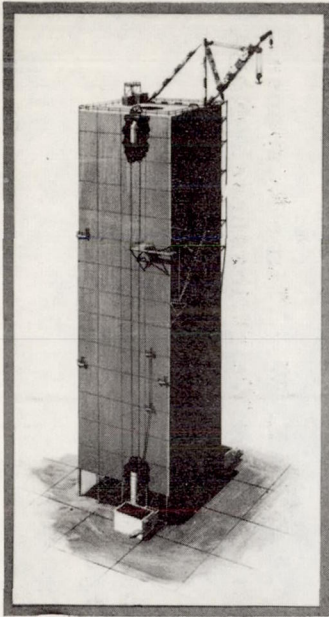
It was concluded that the errors in acceleration accuracy due to the thruster system should have had a negligible effect on the interface shapes. The maximum error should have been 3% and such a variation in Bond number insignificantly influences the interface, especially for the Bond number range tested. Therefore, the greatest source of error in the experimental data probably resulted from the reflections, distortions, shadows, etc., that occurred whenever the interface took shape.



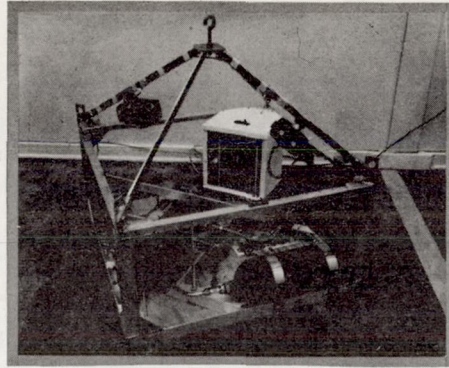
## REFERENCES

1. McAnelly, W. B.; Covington, W. J.: Low Gravity Fluid Mechanics and Thermodynamics Experiments in a Drop Tower Facility. NASA TMX 53765.
2. Bradley, D.; Vaughn, J. E.: Simulation of a Facility for Zero and Low Gravity Environments. Space Division of Chrysler Corporation, Technical Report No. HSM-R32-67, May 1, 1967.
3. Hastings, L.; Rutherford, R.: Low Gravity Liquid-Vapor Interface Shapes in Axisymmetric Containers and a Computer Solution. NASA TMX 53790, October 1968.
4. Wood, G. B.: Zero-G Report-Liquid-Liquid Model. General Dynamics/Astronautics Division of Convair Report 55D859-9, May 1962.
5. Olsen, W. A.: Simulator for Static Liquid Configuration in Propellant Tanks Subject to Reduced Gravity. NASA TN D-3249, May 1966.
6. Paynter, H. L.: Time for a Totally Wetting Liquid to Deform from a Gravity-Dominated to a Nulled-Gravity Equilibrium State. AIAA Journal, Vol. 2, No. 9, December 1964, p. 1627.
7. Fung, F. W.: Dynamic Response of Liquids in Partially Filled Containers Suddenly Experiencing Weightlessness. Symposium on Fluid Mechanics and Heat Transfer Under Low Gravitational Conditions, Lockheed Missiles and Space Company, June 24 - 25, 1965.
8. Siegret, C. E.; Petrash, D. A.; Otto, E. W.: Time Response of Liquid-Vapor Interface After Entering Weightlessness. NASA TN D-2458, 1964.
9. Benedikt, E. T.: Scale of Separation Phenomena in Liquids Under Conditions of Nearly Free Fall. ARS Journal, Vol. 29, No. 2, February 1959, pp. 150 - 151.
10. Reid, W. H.: Oscillations of a Viscous Liquid Droplet. Tech. Rept. No. 32, Div. of Appl. Mech., Brown University, 1960.





Saturn V Dynamic Test Stand



Low Gravity Experimental Package

### Capabilities

#### Payload

Present \_\_\_\_\_ 450 lb  
 Future \_\_\_\_\_ 1000 lb

#### Low Gravity Test Range

Minimum \_\_\_\_\_  $10^{-5} g_0$   
 Maximum \_\_\_\_\_  $4 \times 10^{-2} g_0$

Drop Time (294') \_\_\_\_\_ 4.135 sec

Total Drop Weight \_\_\_\_\_ 4000 lb

Maximum Test Package \_\_\_\_\_ 3 ft dia. x 3 ft high

Deceleration \_\_\_\_\_ Less Than 25 g's

Telemetry Instrumentation \_\_\_\_\_ 20 Channel

Non-Destructive Testing

Zero Turn-Around Time

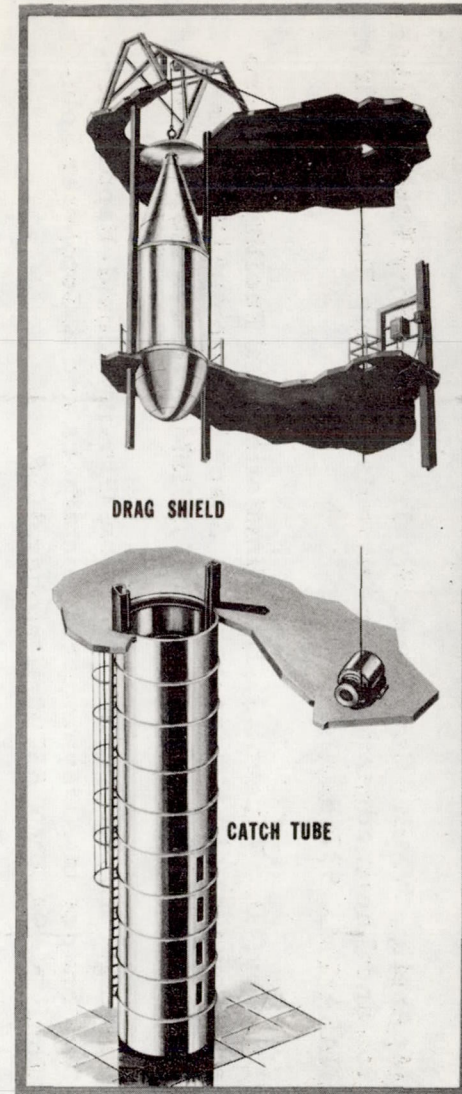


FIGURE 1. MARSHALL SPACE FLIGHT CENTER DROP TOWER FACILITY



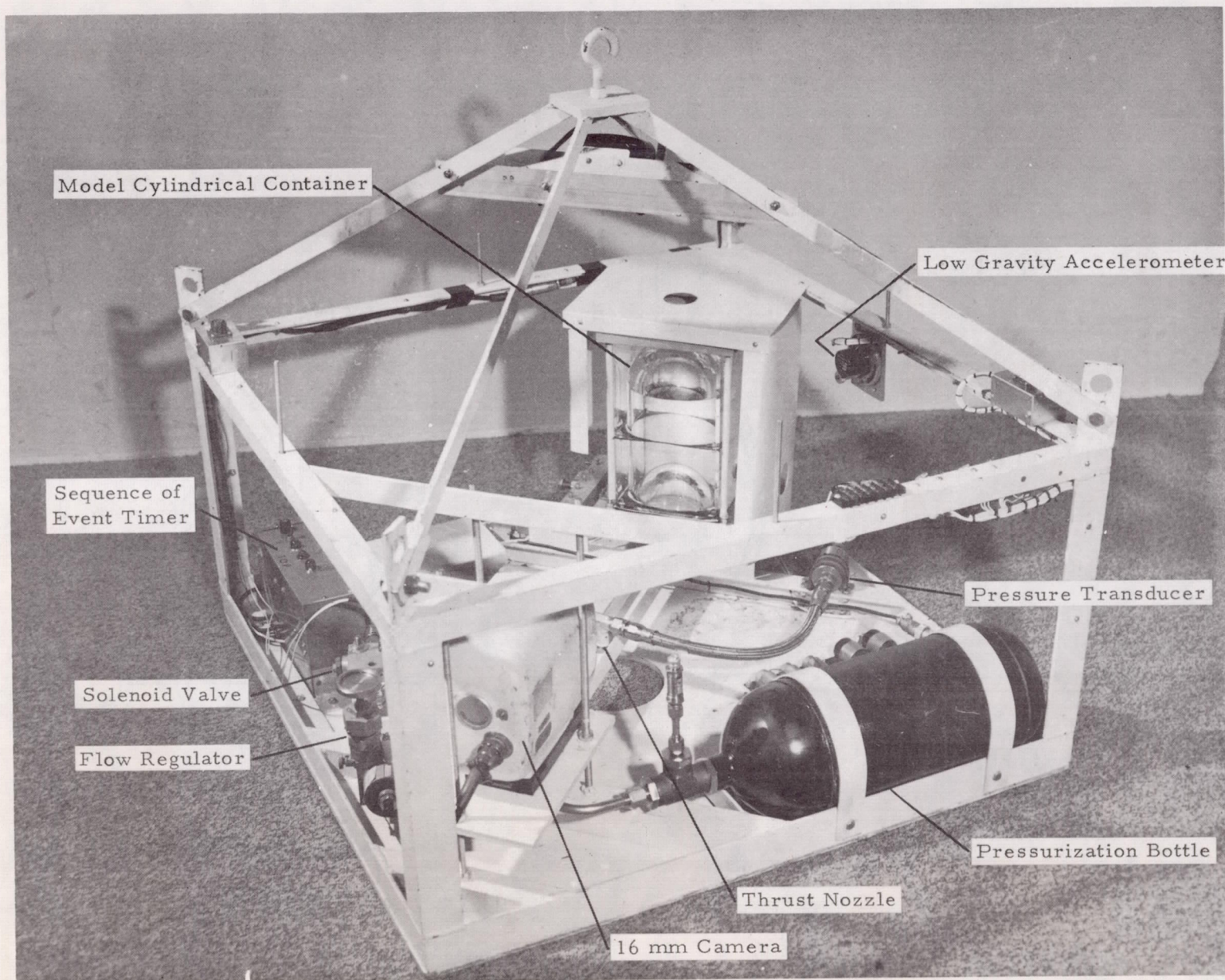


FIGURE 2 . EXPERIMENTAL DROP TOWER PACKAGE



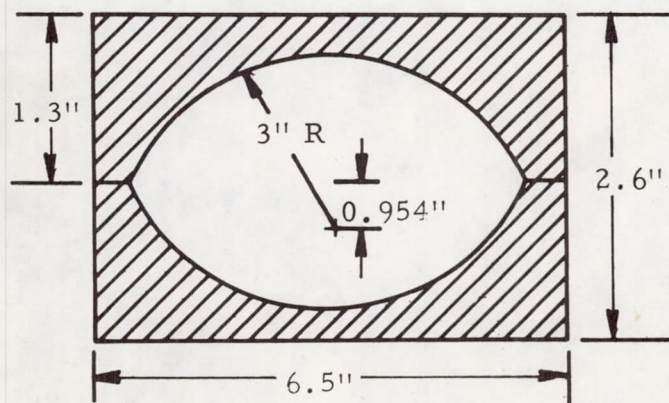
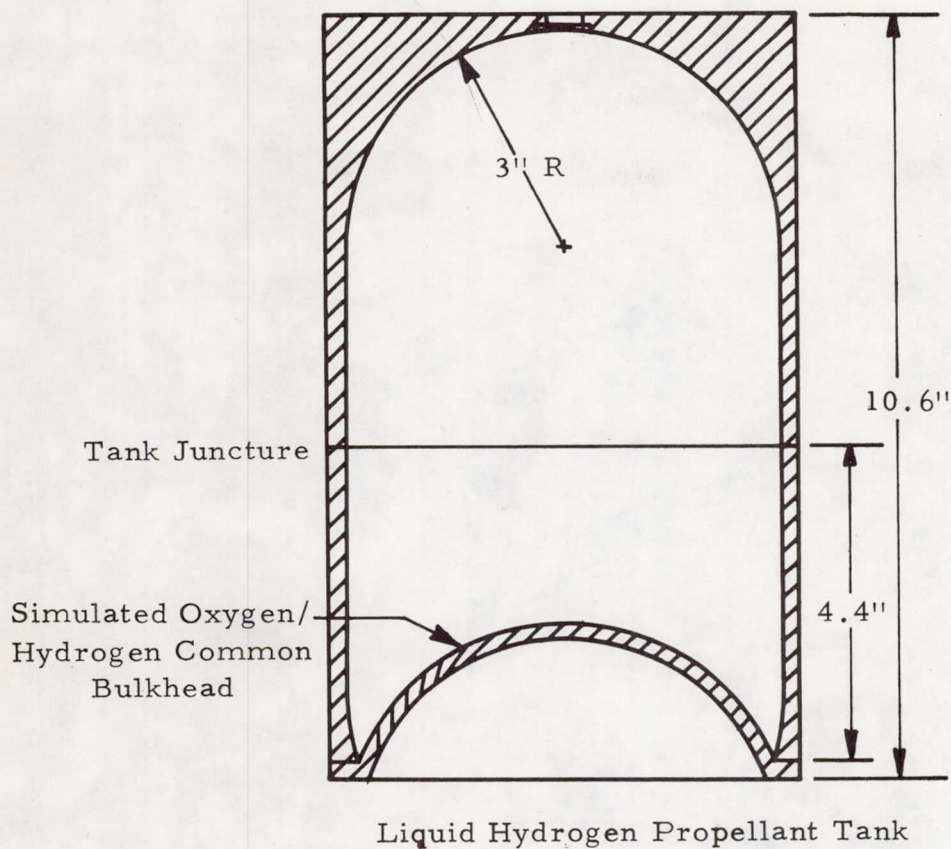


FIGURE 3. MODEL SATURN V/S-IVB PROPELLANT CONTAINERS



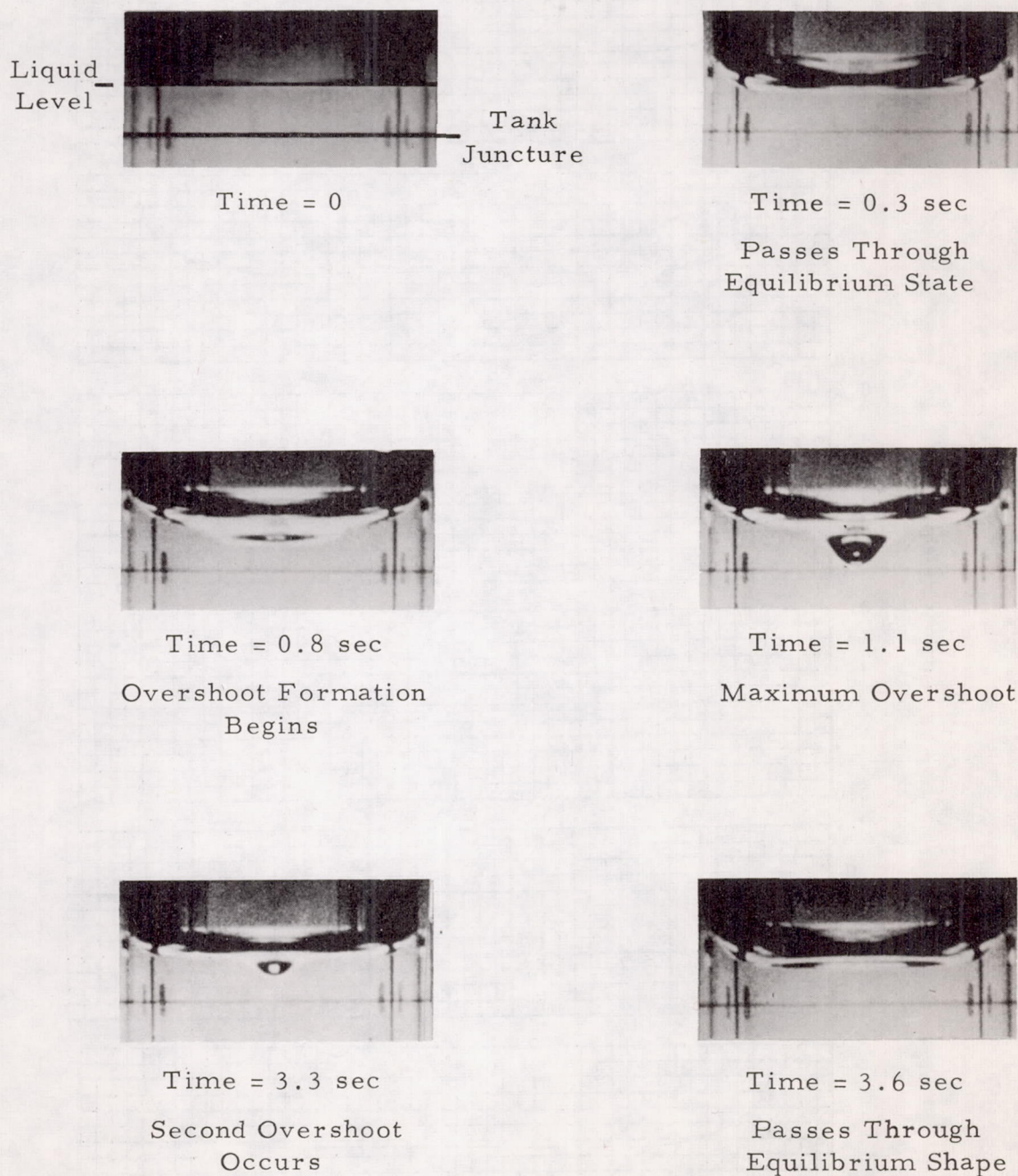


FIGURE 4. EXPERIMENTAL INTERFACE SHAPES IN A CYLINDER  
AT BOND NO. = 48



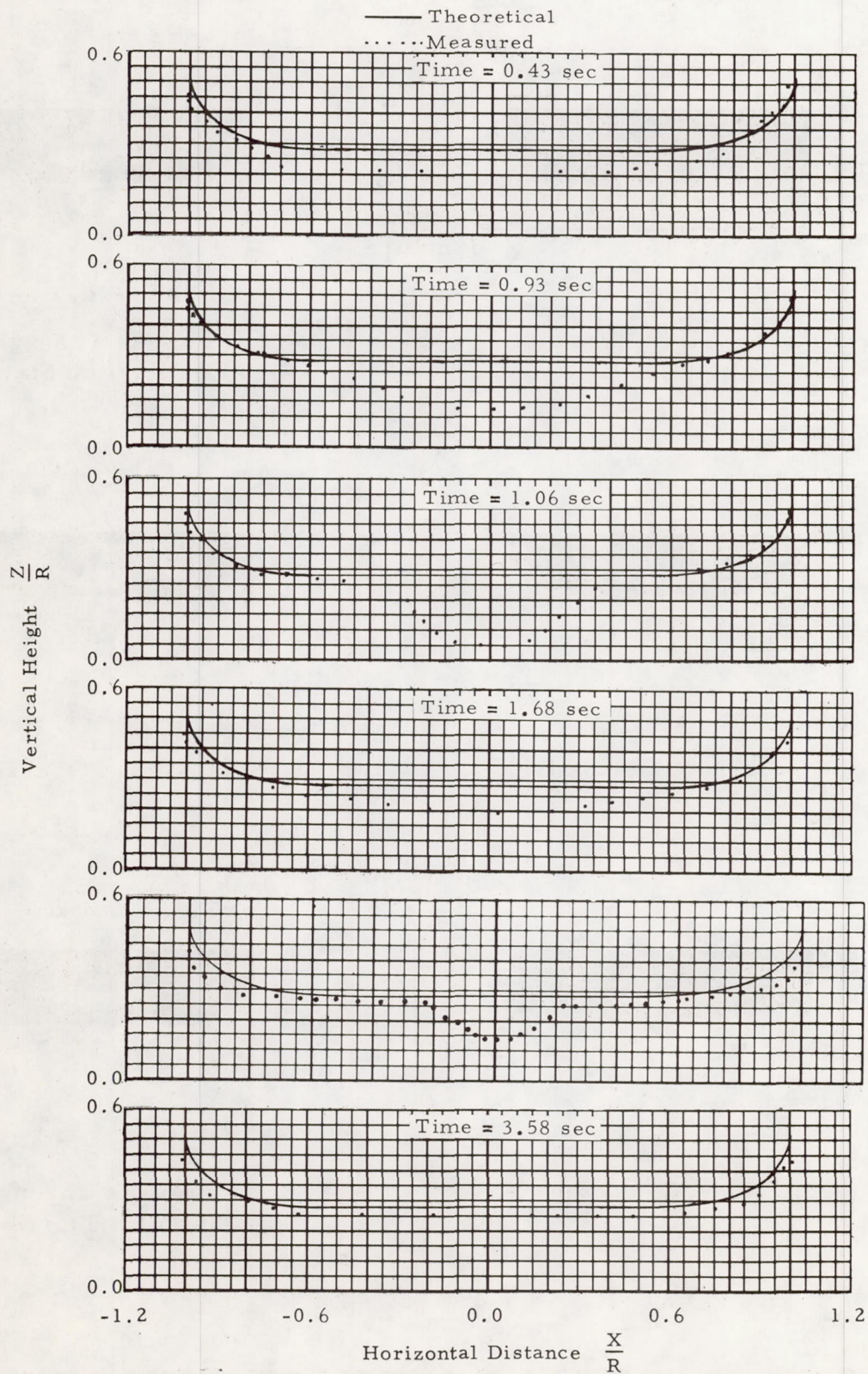


FIGURE 5. EXPERIMENTAL INTERFACE SHAPES IN A CYLINDER AT BOND NUMBER = 48



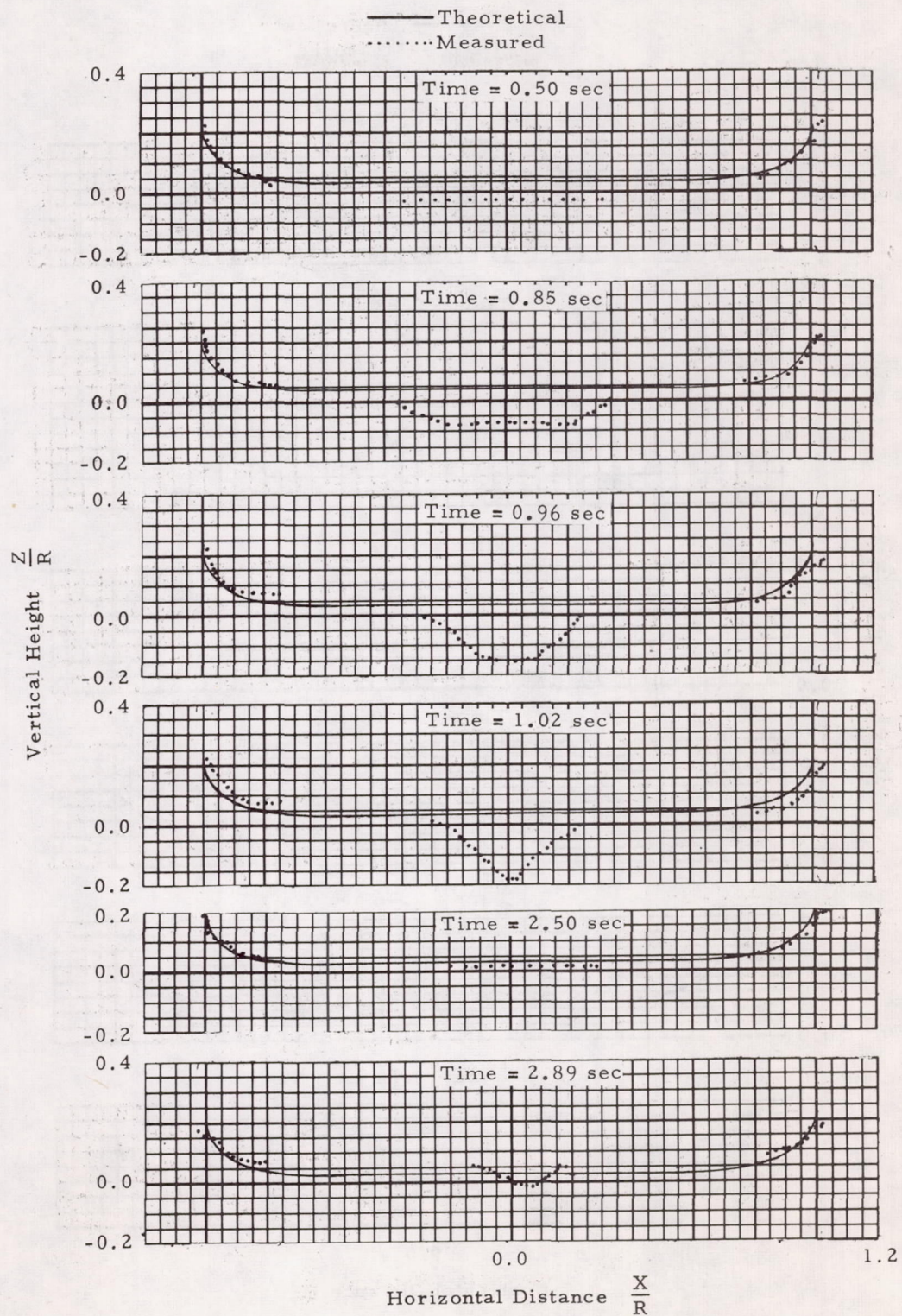


FIGURE 6. EXPERIMENTAL INTERFACE SHAPES IN A CYLINDER AT BOND NUMBER = 80



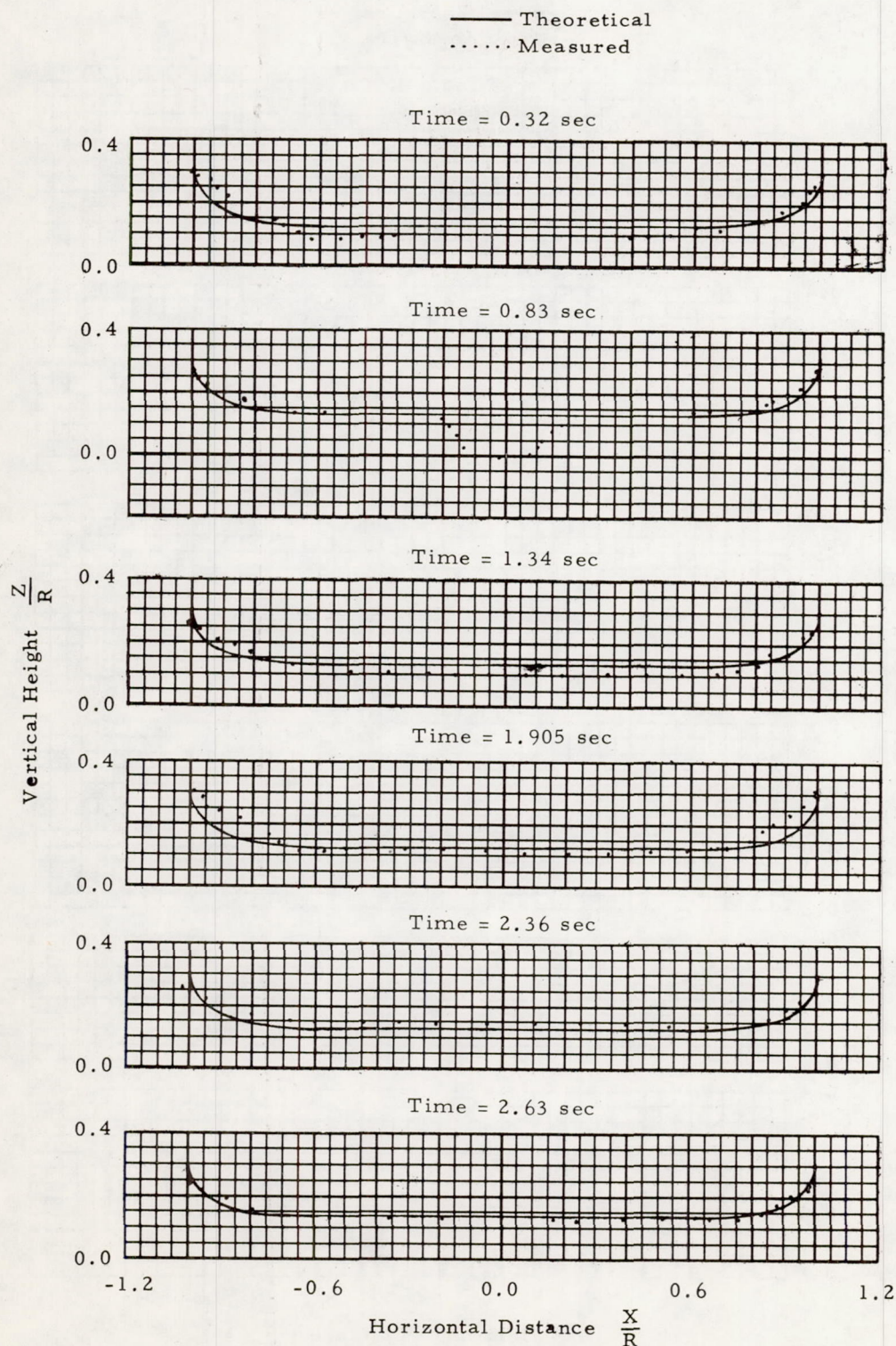
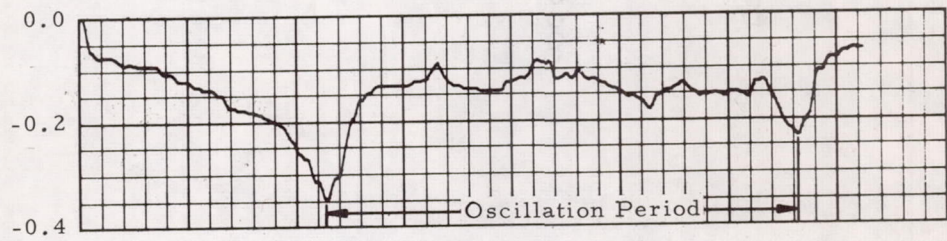


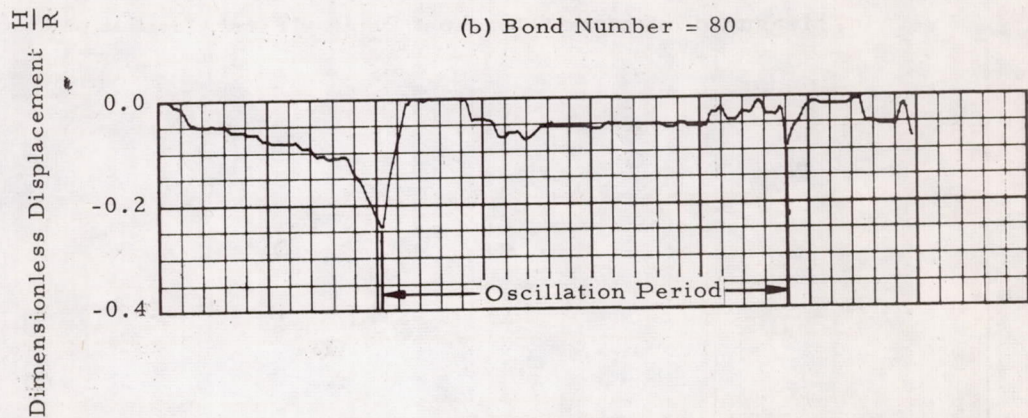
FIGURE 7. EXPERIMENTAL INTERFACE SHAPES IN A CYLINDER  
AT BOND NUMBER = 94



(a) Bond Number = 48



(b) Bond Number = 80



(c) Bond Number = 94

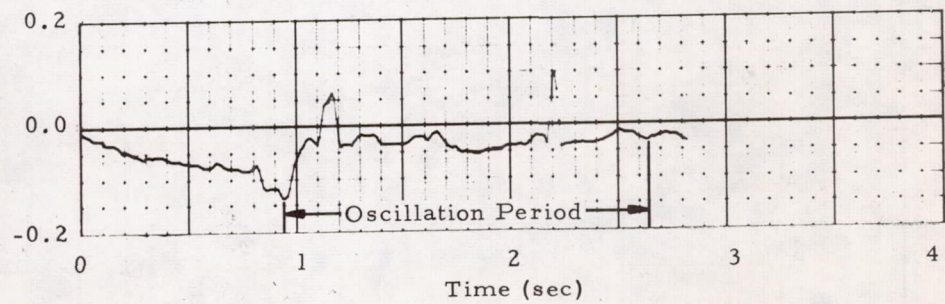


FIGURE 8. MEASURED DISPLACEMENT OF INTERFACE CENTERPOINT IN A CYLINDER VERSUS TEST TIME



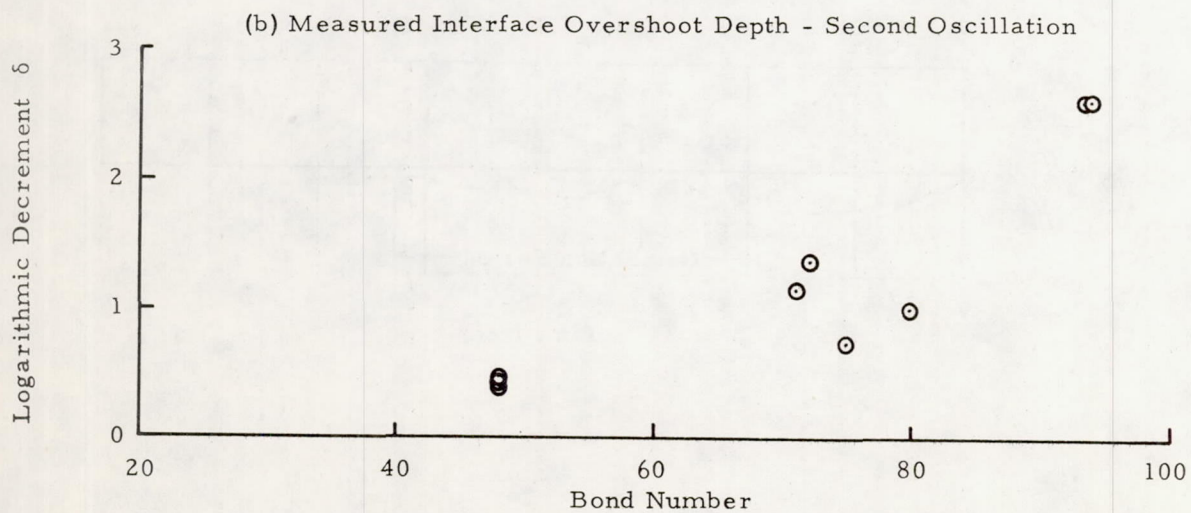
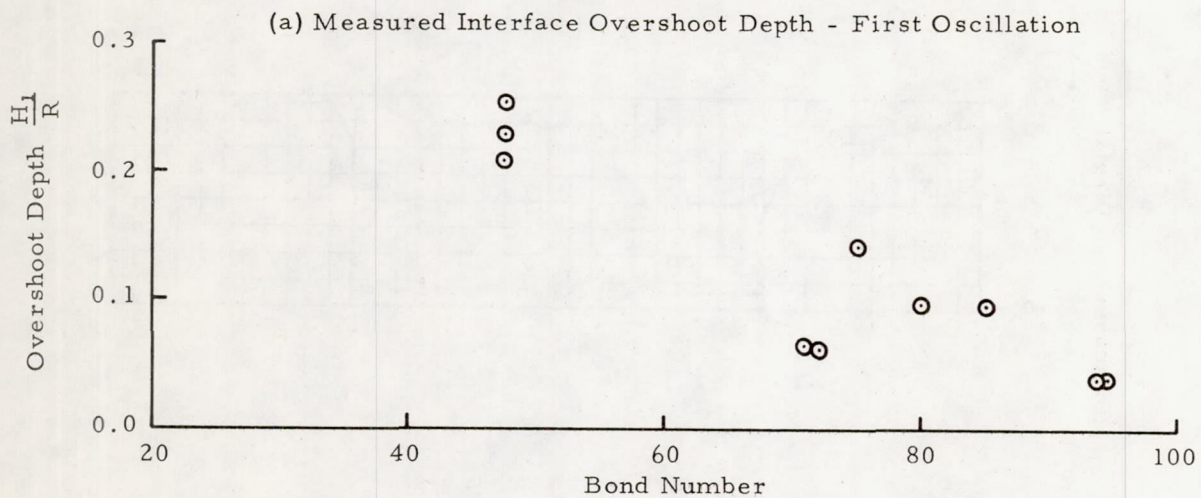
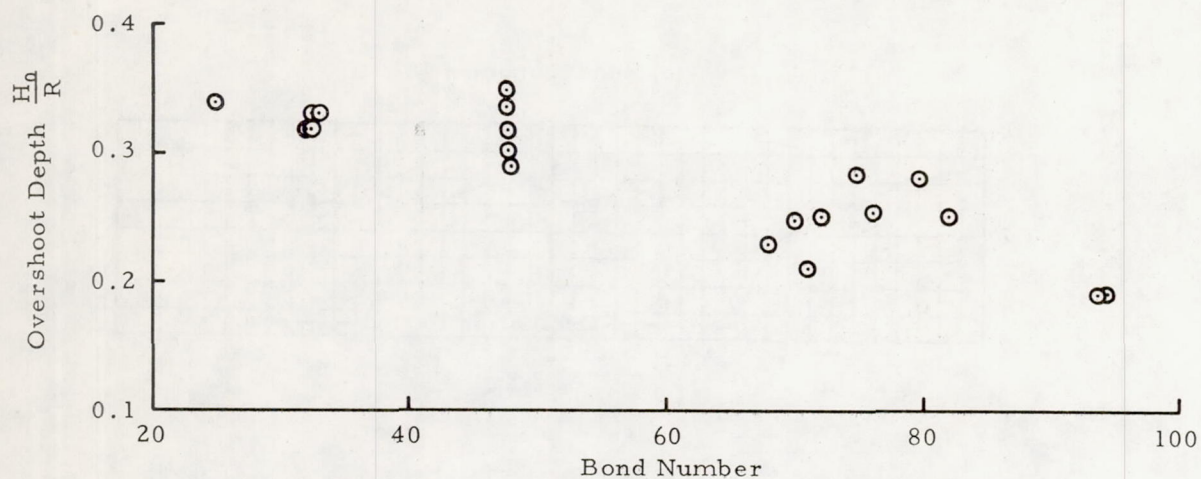


FIGURE 9. MEASURED INTERFACE OSCILLATORY MAGNITUDES IN A CYLINDER SIX INCHES IN DIAMETER



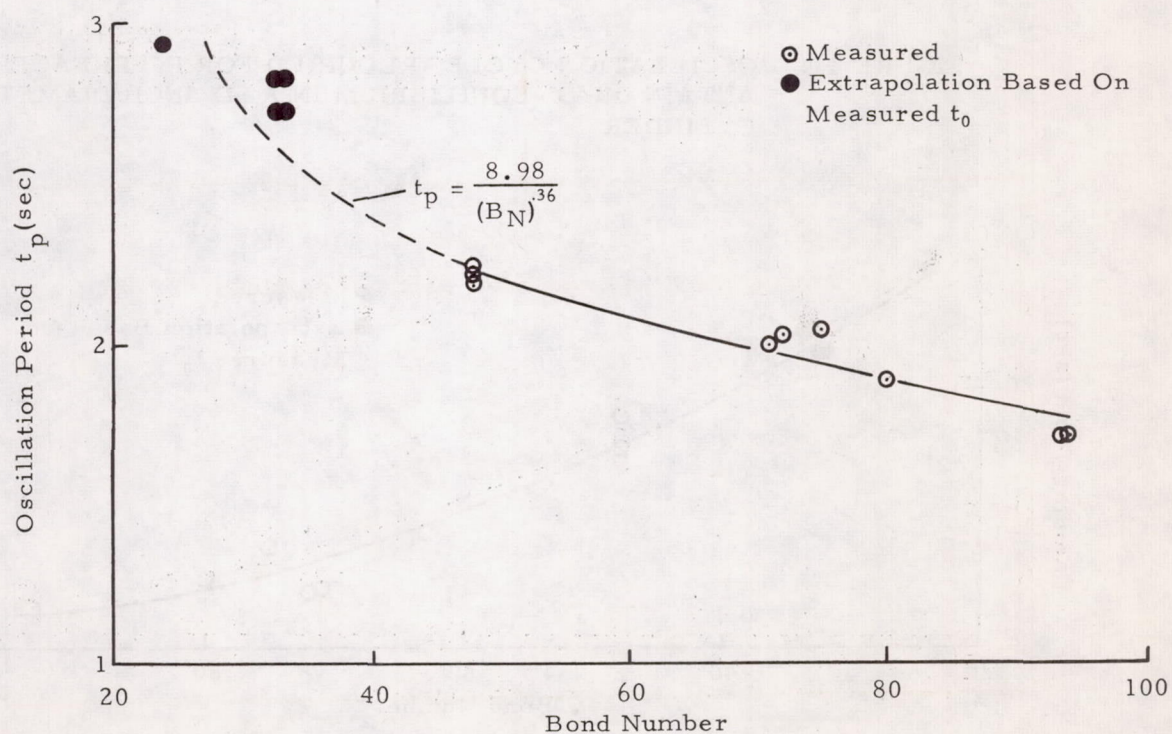
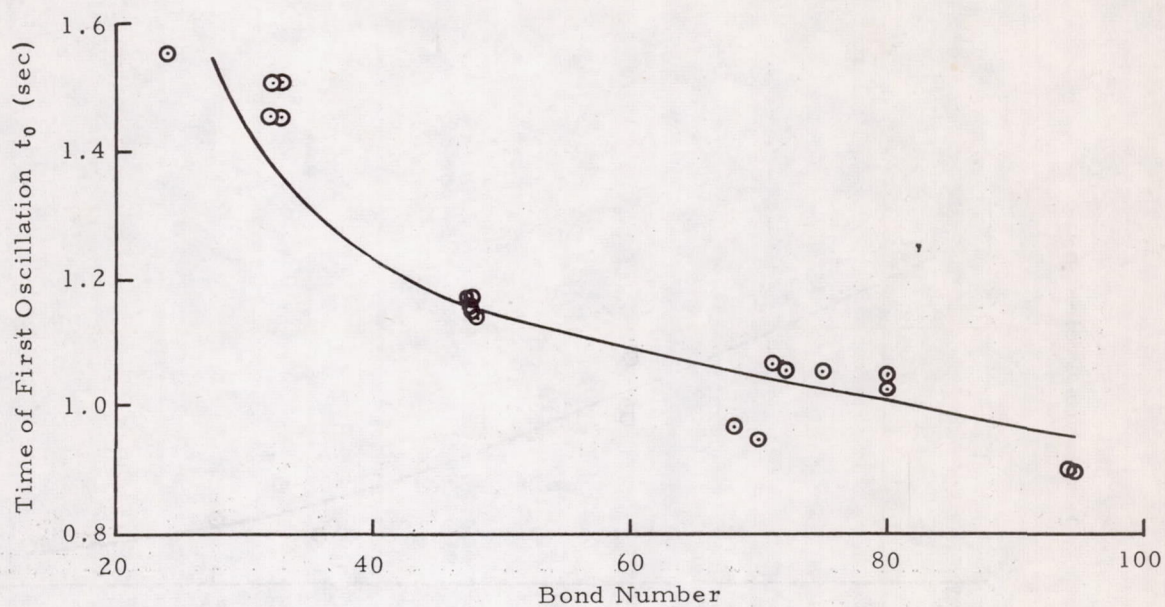


FIGURE 10. MEASURED TIMES CHARACTERISTIC OF INTERFACE FORMATION DYNAMICS IN A CYLINDER SIX INCHES IN DIAMETER



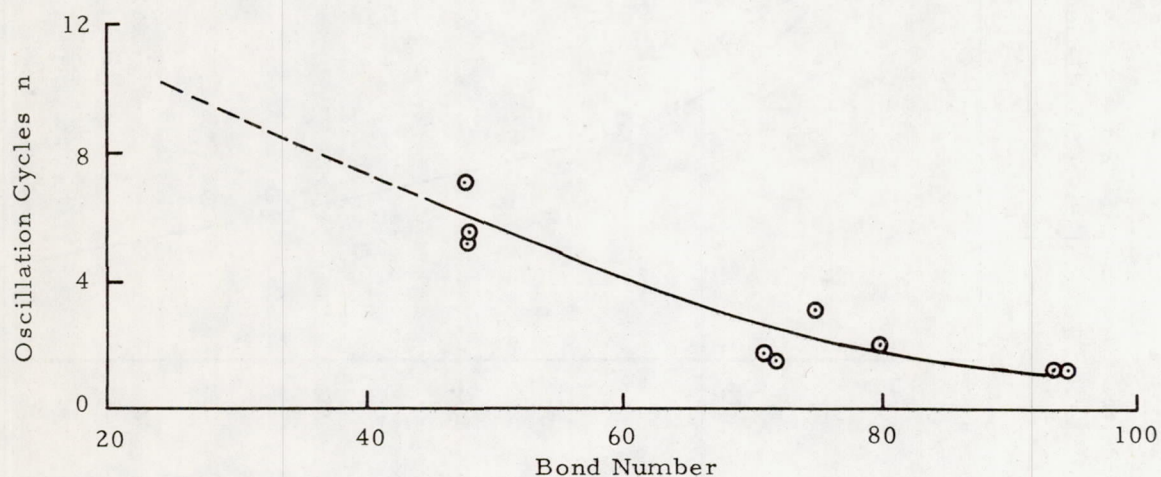


FIGURE 11. OSCILLATION CYCLES REQUIRED FOR INTERFACE TO ATTAIN QUASI-EQUILIBRIUM IN A SIX INCH DIAMETER CYLINDER

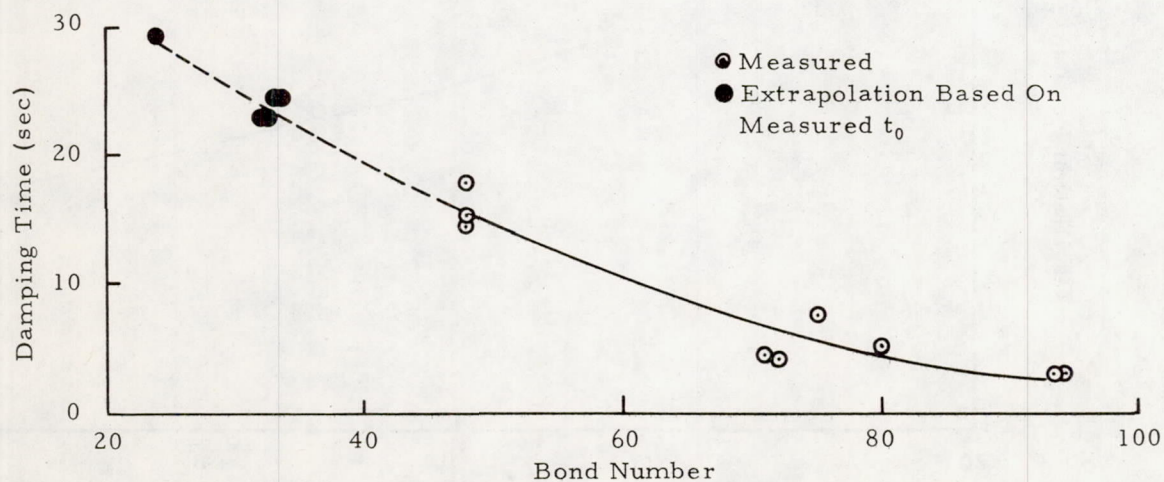


FIGURE 12. TOTAL TIME REQUIRED FOR INTERFACE TO ATTAIN QUASI-EQUILIBRIUM IN A SIX INCH DIAMETER CYLINDER



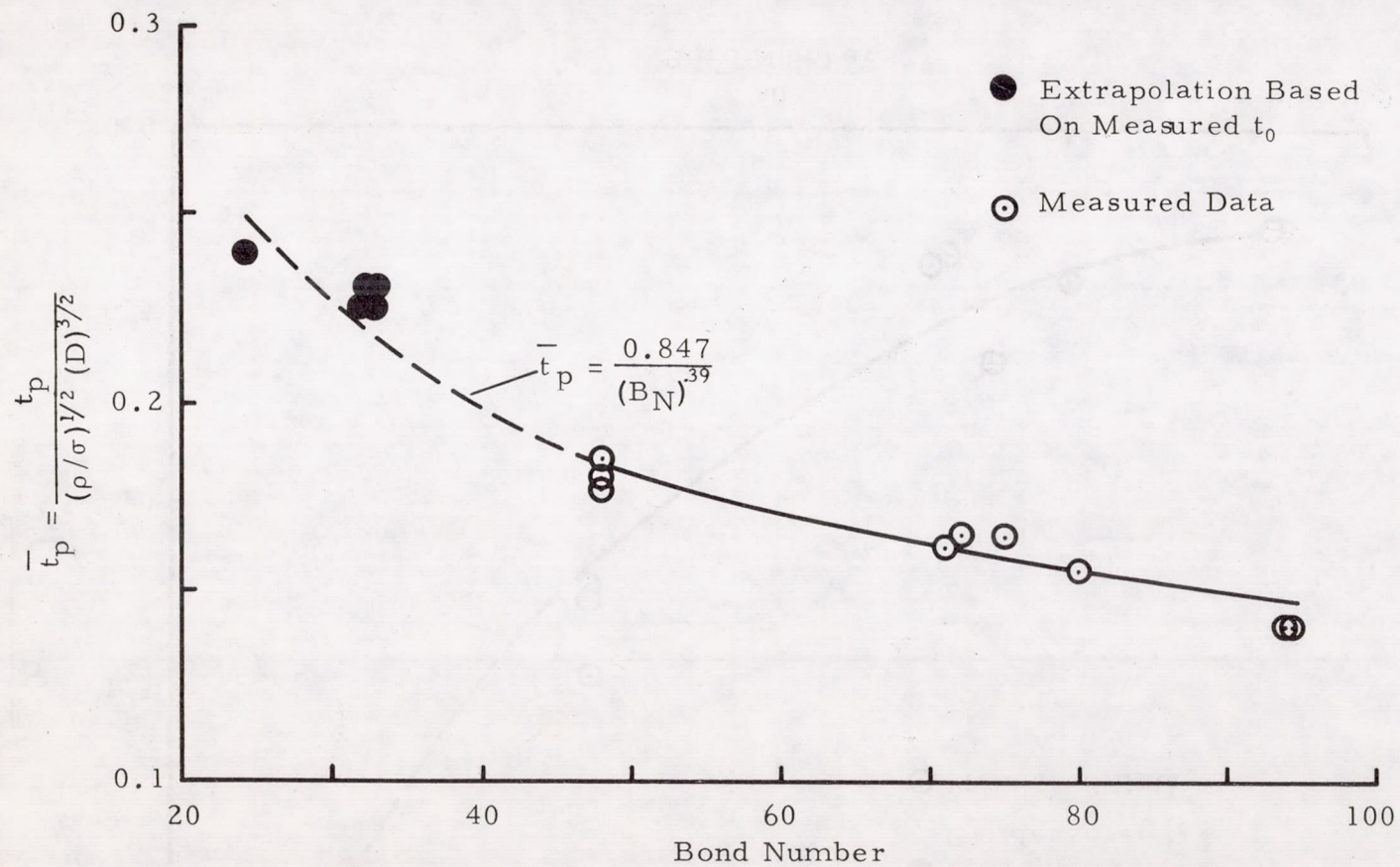


FIGURE 13. NON-DIMENSIONALIZED INTERFACE OSCILLATION PERIOD IN A CYLINDER VERSUS BOND NUMBER



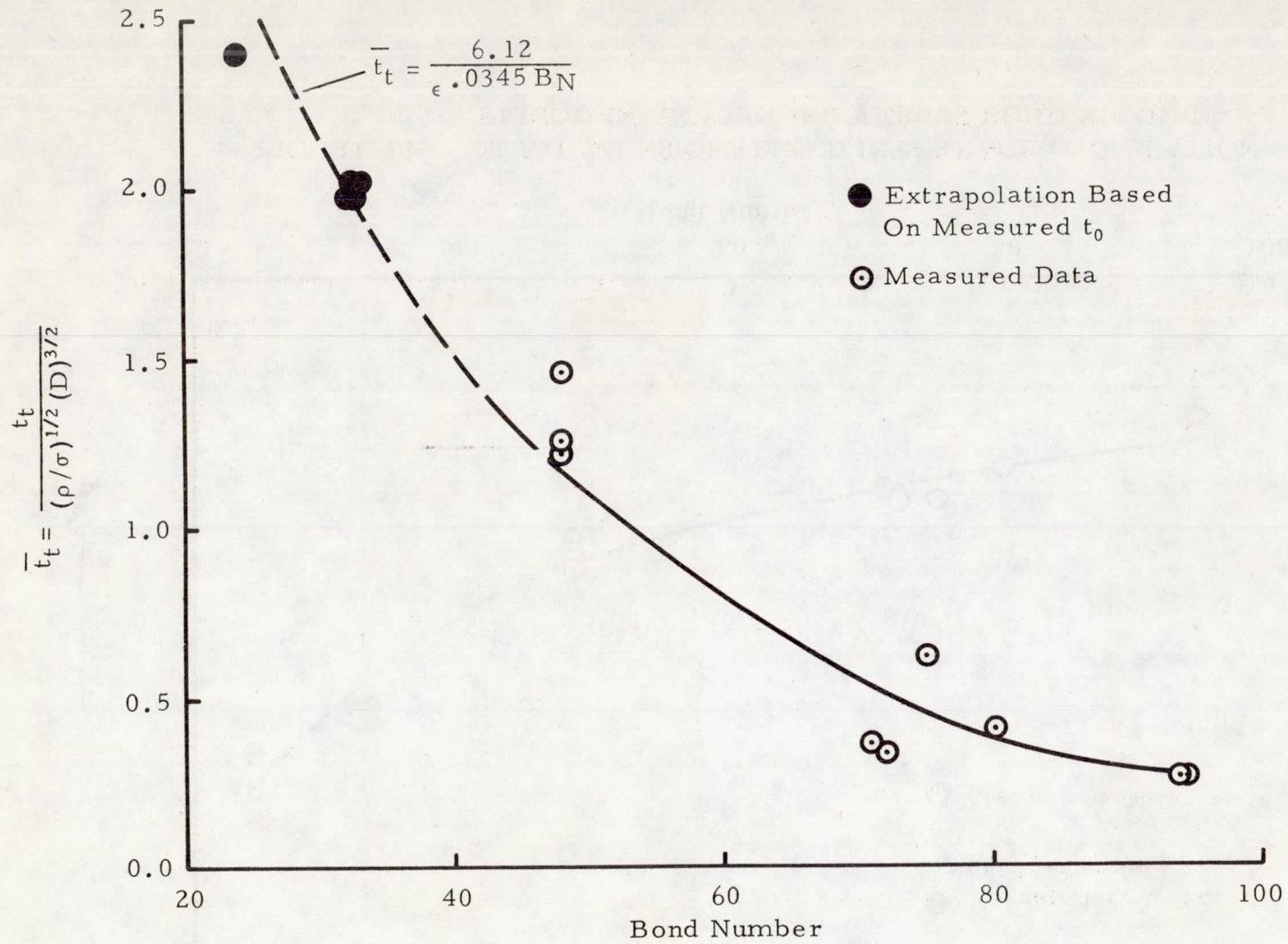


FIGURE 14. NON-DIMENSIONALIZED TIME REQUIRED FOR INTERFACE TO ATTAIN QUASI-EQUILIBRIUM IN A CYLINDER VERSUS BOND NUMBER



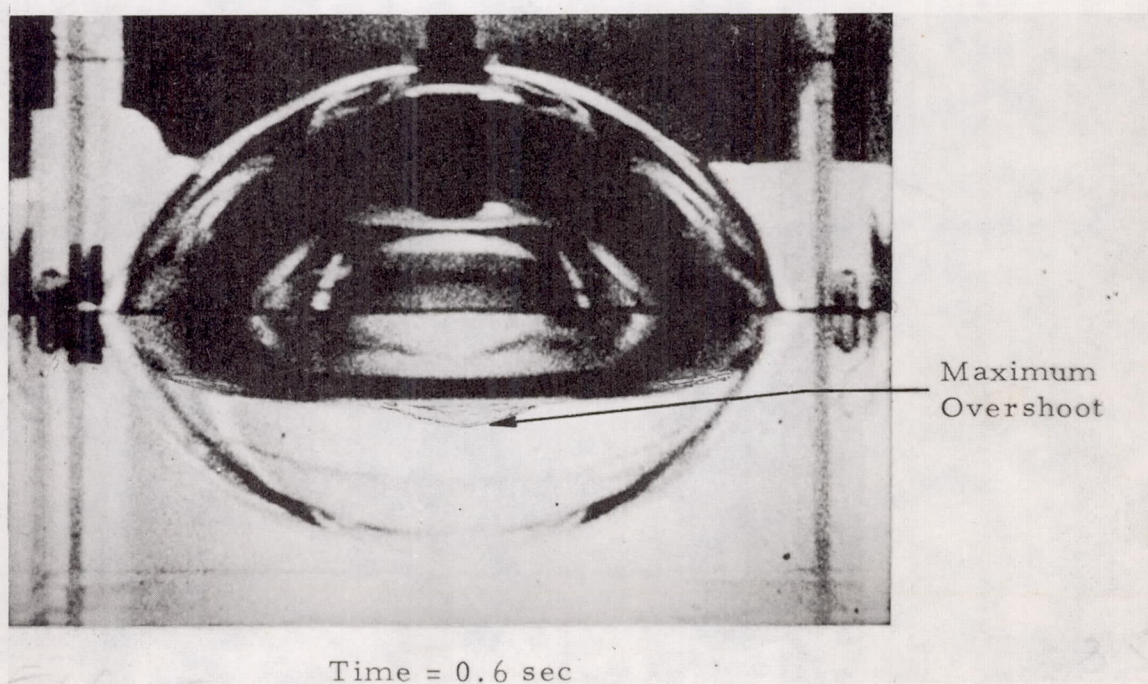
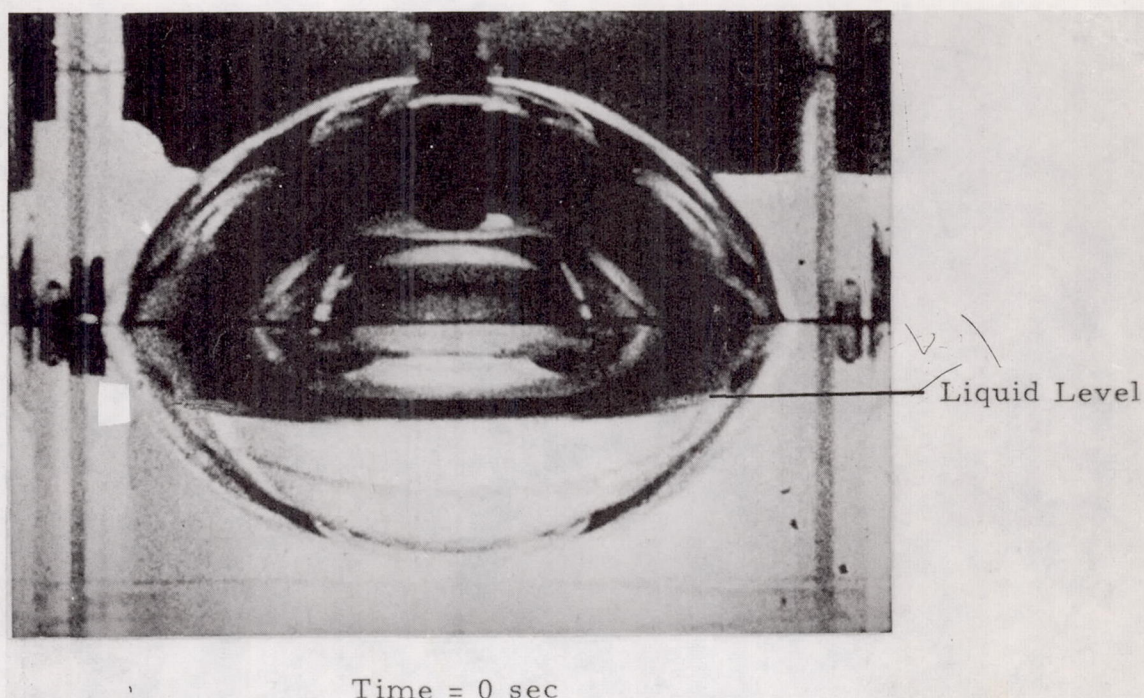


FIGURE 15 . EXPERIMENTAL INTERFACE FORMATION DYNAMICS  
CHARACTERISTIC OF A SPHERE AT BOND NO. = 80



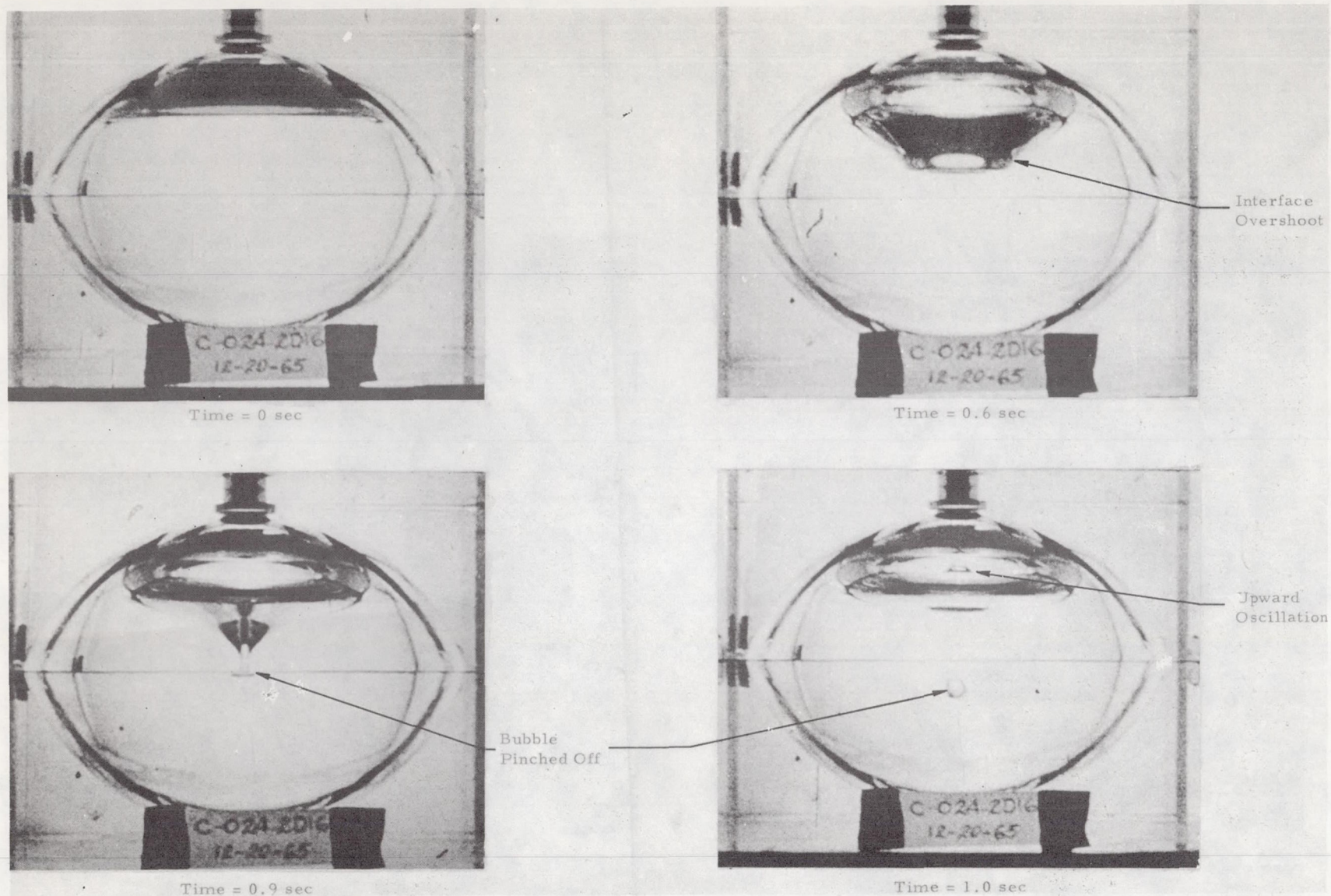


FIGURE 16. INTERFACE FORMATION DYNAMICS CHARACTERISTIC OF A SPHERE AT BOND NO. = 80



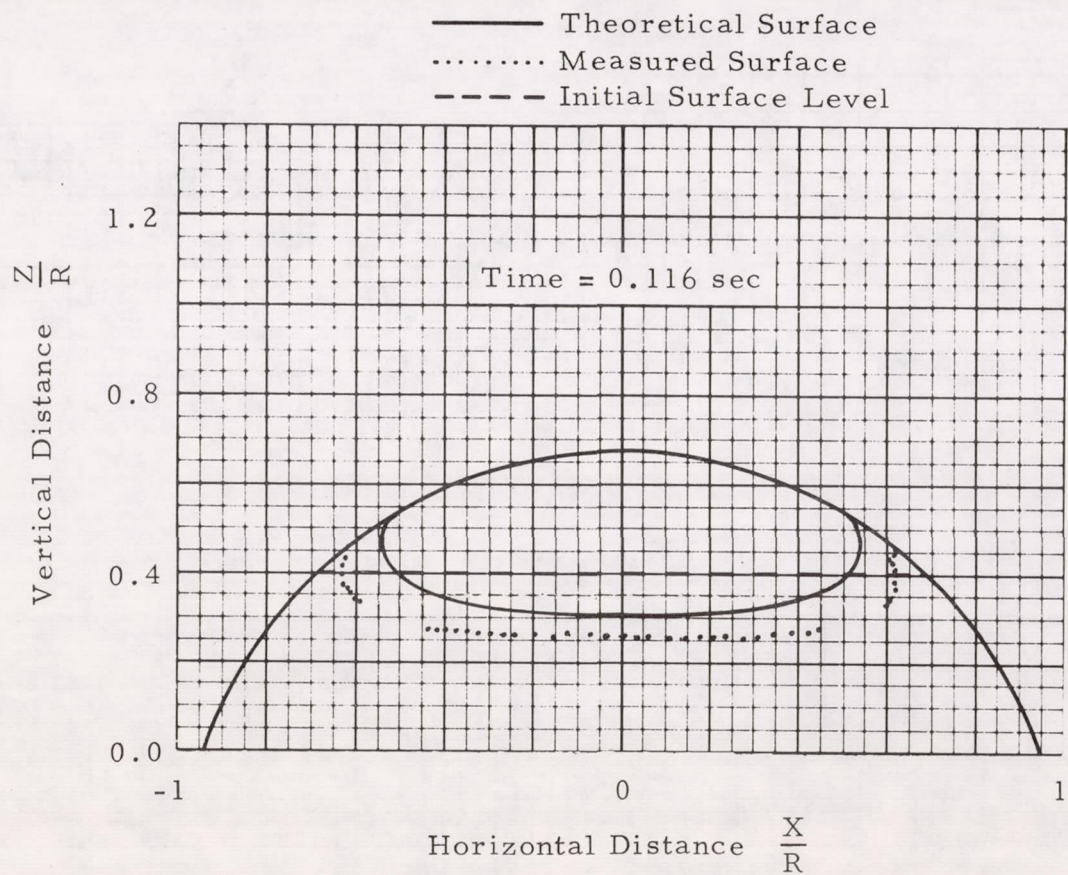


FIGURE 17a. EXPERIMENTAL INTERFACE FORMATION IN A SPHERICAL SEGMENT AT BOND NUMBER = 80



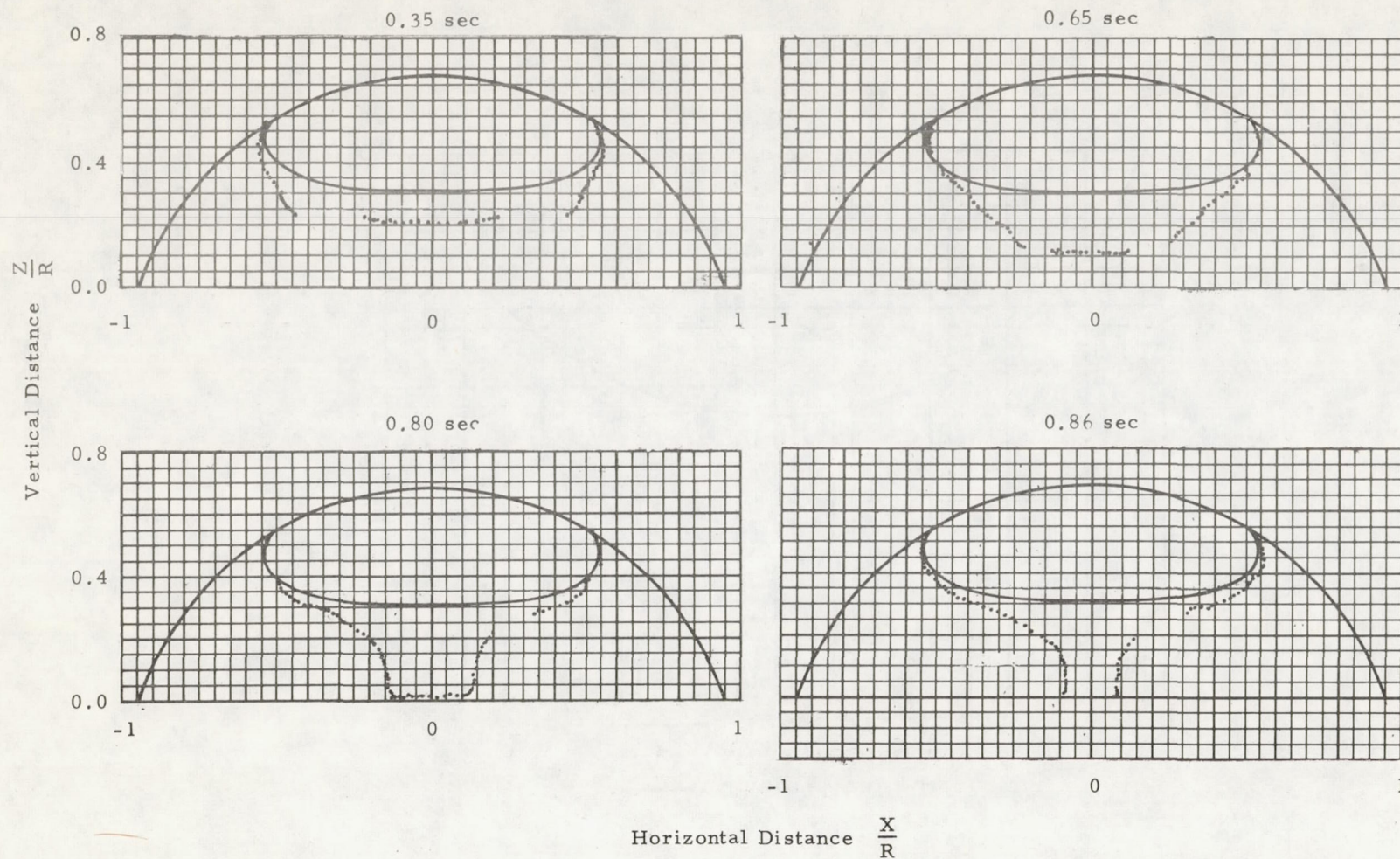


FIGURE 17b. EXPERIMENTAL INTERFACE FORMATION IN A SPHERICAL SEGMENT AT BOND NUMBER = 80



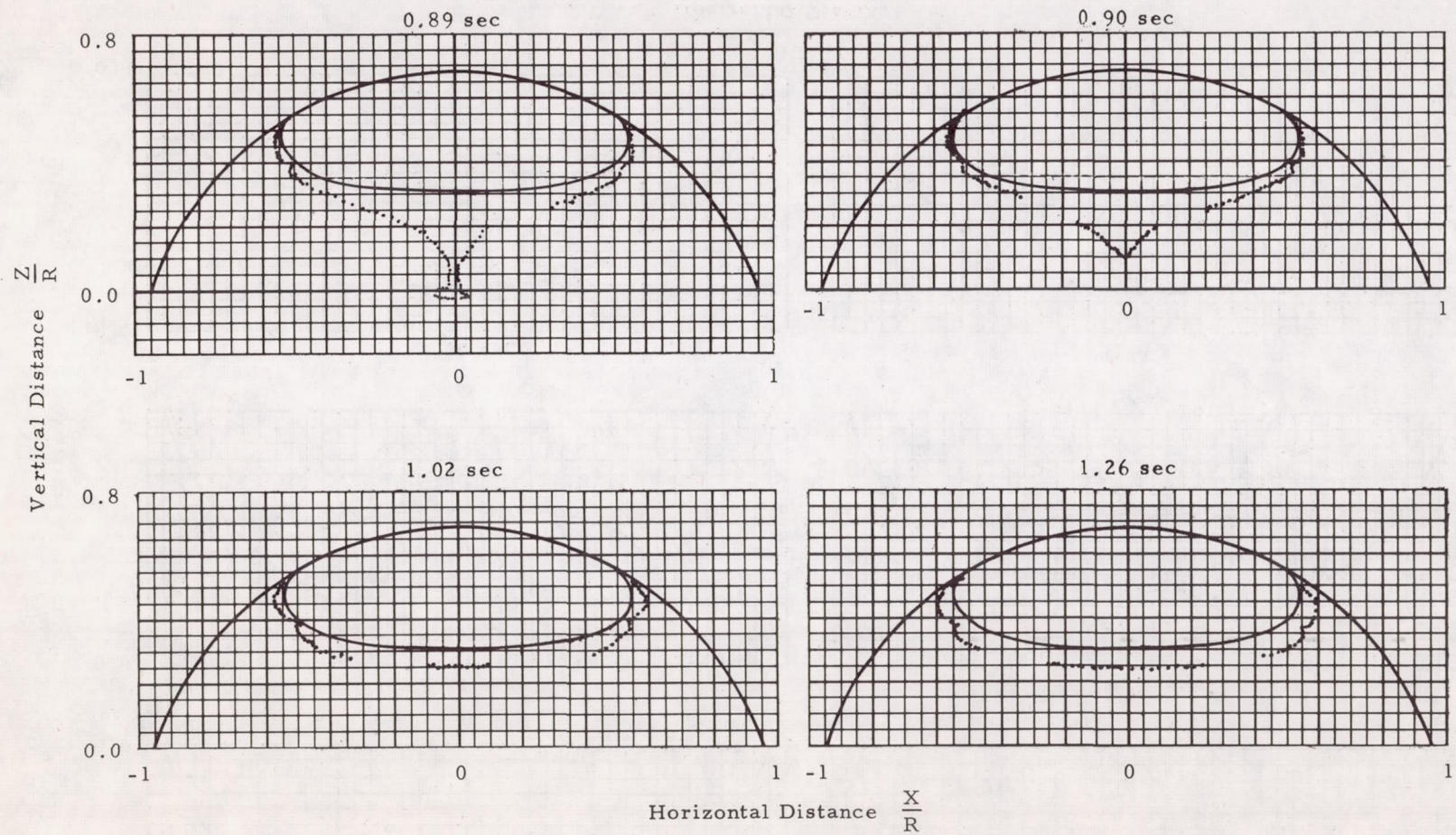


FIGURE 17c. EXPERIMENTAL INTERFACE FORMATION IN A SPHERICAL SEGMENT AT BOND NUMBER = 80



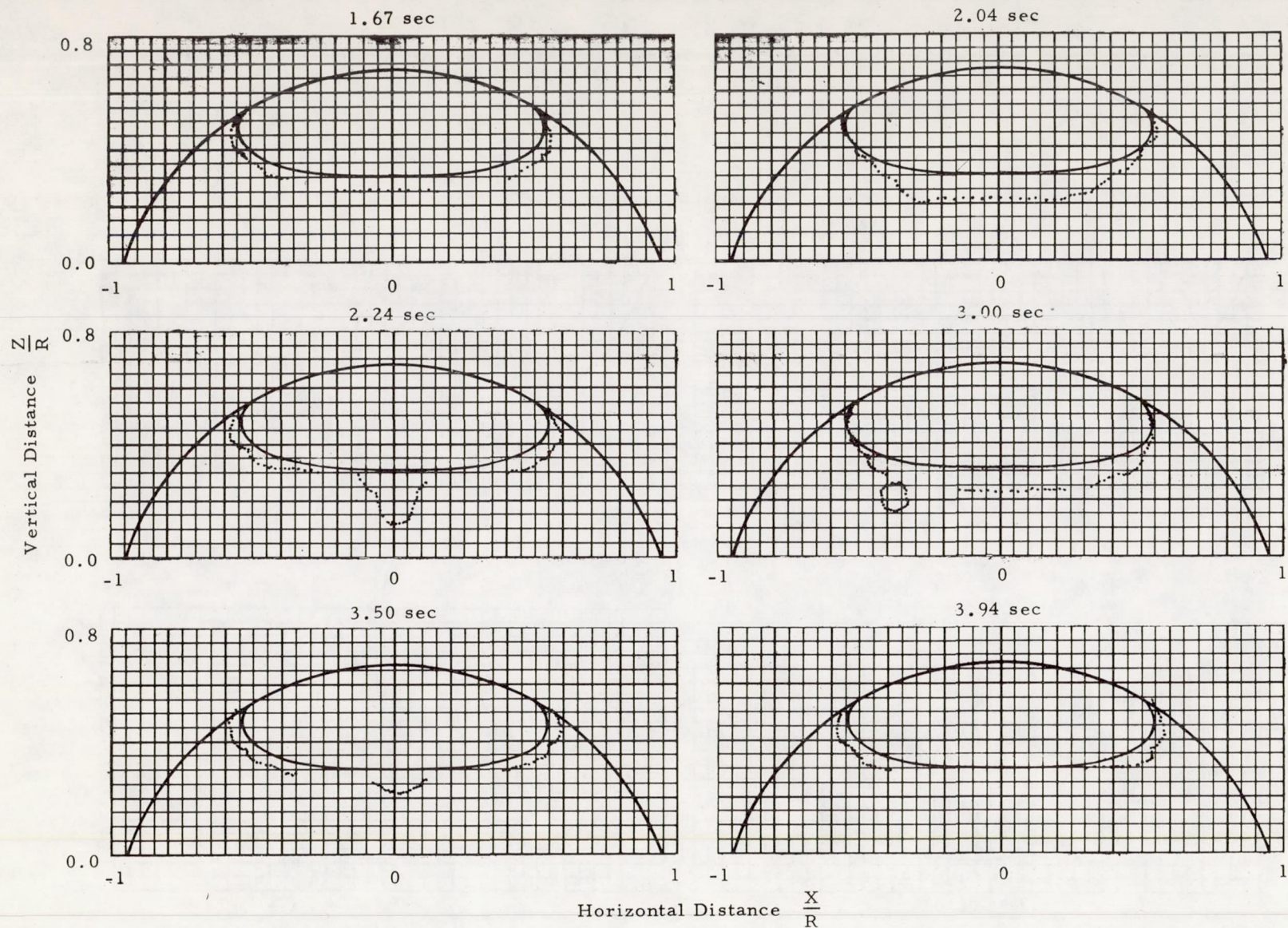


FIGURE 17d. EXPERIMENTAL INTERFACE FORMATION IN A SPHERICAL SEGMENT AT BOND NUMBER = 80



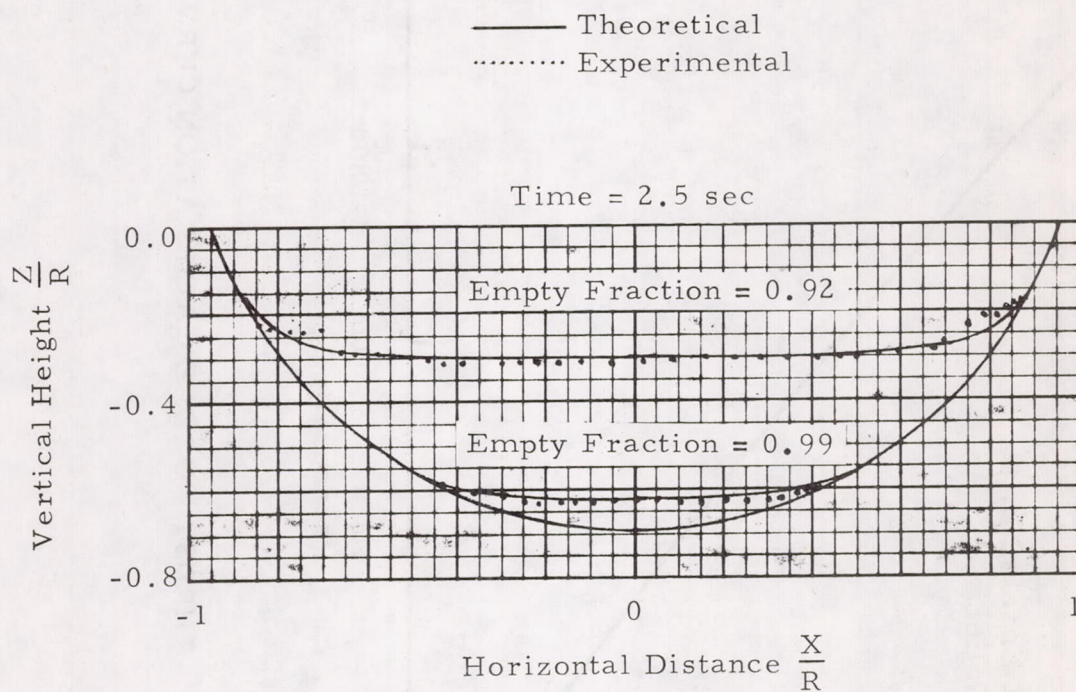


FIGURE 18. EXPERIMENTAL INTERFACE SHAPES IN A SPHERICAL SEGMENT AT BOND NUMBER = 80



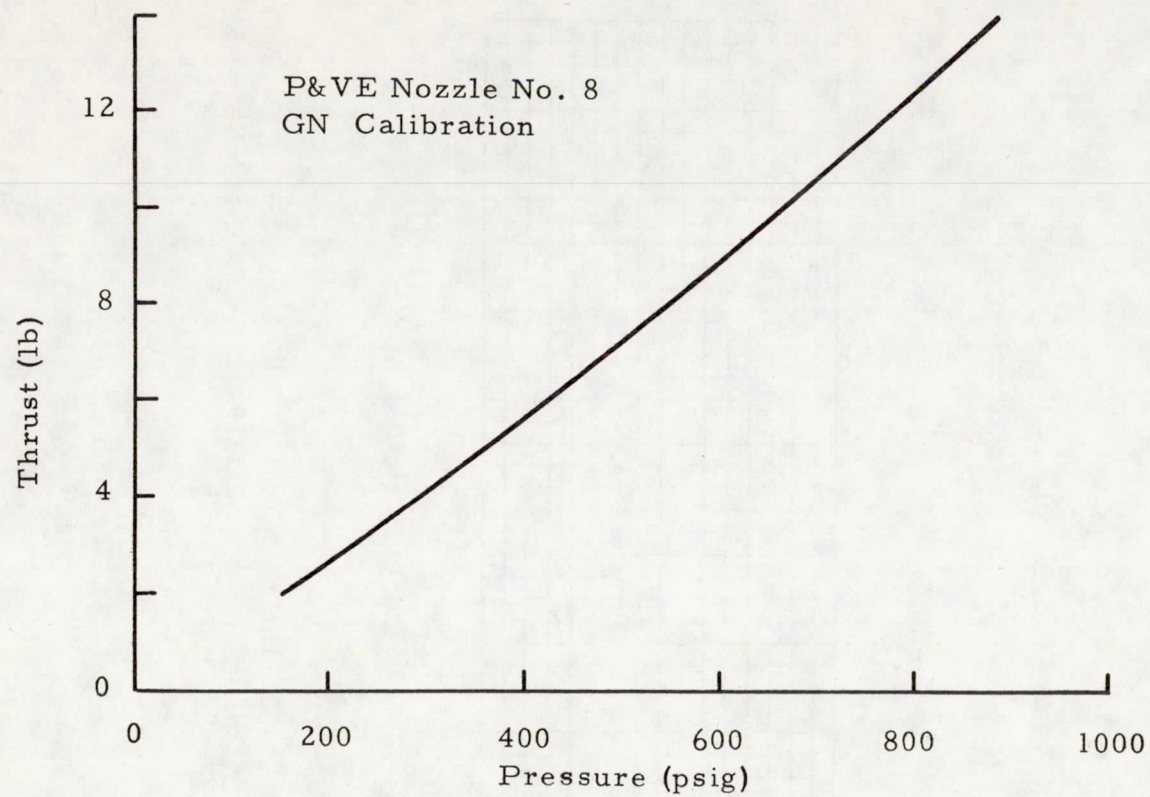


FIGURE 19. THRUST NOZZLE CALIBRATION CURVE



EXPERIMENTAL STUDY OF THE RESPONSE  
OF A  
STATIC LIQUID-VAPOR INTERFACE  
AFTER A SUDDEN REDUCTION IN ACCELERATION

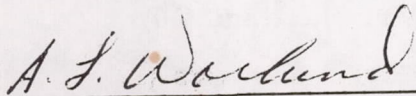
By Leon J. Hastings

The information in this report has been reviewed for security classification. Review of any information concerning Department of Defense or Atomic Energy Commission programs has been made by the MSFC Security Classification Officer. This report, in its entirety, has been determined to be unclassified.

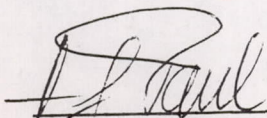
This document has also been reviewed and approved for technical accuracy.



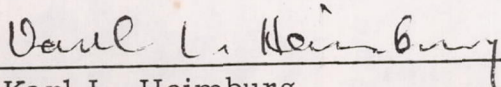
L. J. Hastings  
Chief, Fluid Mechanics Section



A. L. Worlund  
Chief, Fluid Mechanics and Dynamics  
Branch



H. G. Paul  
Chief, Propulsion and Thermodynamics  
Division



Karl L. Heimburg  
Director, Astronautics Laboratory



## DISTRIBUTION

DIR  
DEP-T  
PM-DIR  
PD-DIR

S&E-DIR

S&E-AERO-DIR  
S&E-COMP-RR  
S&E-ASTN-DIR  
S&E-ASTN-T

S&E-ASTN-TF  
S&E-ASTN-TFM  
S&E-ASTN-S

S&E-ASTN-EM  
S&E-ASTN-RM  
S&E-ASTN-P

S&E-ASTN-PL  
S&E-ASTN-PT  
S&E-ASTN-PF  
S&E-ASTN-PFA

A&TS-PAT  
PM-PR  
A&TS-MS-H  
A&TS-MS-IP  
A&TS-MS-IL (8)  
A&TS-TU (6)

Scientific and Technical Information Facility (25)  
Attn: NASA Representative (S-AK/RKT)  
P. O. Box 33  
College Park, Maryland 20740

Dr. von Braun  
Dr. Rees  
General O'Connor  
Dr. Lucas  
Dr. Mrazek  
Dr. Weidner  
Mr. Williams  
Dr. Geissler  
Mr. R. Craft (2)  
Mr. Heimbürg  
Mr. Grafton  
Mr. Goetz  
Mr. Perry  
Mr. Stone  
Mr. Isbell  
Mr. Beduerftig  
Mr. Fuhrmann  
Miss Scott  
Mr. Paul  
Mr. Wood  
Mr. Hopson  
Mr. Vaniman  
Mr. Worlund  
Mr. Hastings (10)



DISTRIBUTION (Concluded)

Brown Engineering, A Teledyne Company  
Huntsville, Alabama

Mr. Duggan, MS-190

Mr. Woods, MS-190

McDonnell Douglas Astronautics Company  
MDAC - Huntsville, Alabama

Bldg. 4481

Attn: Mr. S. L. Zuckerman (3)

Lewis Research Center

21000 Brookpark Road

Cleveland, Ohio 44135

Attn: Mr. E. Otto

Mr. D. Petrash

Manned Spacecraft Center

NASA

Houston, Texas 77058

Attn: J. G. Thibodaux, Chief

Propulsion and Power Division

General Dynamics

P. O. Box 1128

San Diego, California 92112

Attn: R. E. Tatro

Mail Zone: 584-00

Martin-Marietta Corporation

Denver, Colorado 80201

Attn: Mr. Howard Paynter/Dr. T. E. Bowman

Propulsion Research Department

NASA Headquarters

600 Independence Avenue, S. W.

Washington, D. C. 20546

Attn: Mr. J. A. Suddreth (3)

Code RPL

Liquid Propulsion Technology